energies

MDPI

Article

Gradient-Delignified Wood as a Sustainable Anisotropic Insulation Material

Yi Hien Chin [1,2,*], Salah-Eddine Ouldboukhitine [1], Christophe Vial [1], Joseph Gril [1,3], Rostand Moutou Pitti [1,4], Nicolas Labonne [2] and Pascal Biwole [1,5,6,*]

1 Université Clermont Auvergne, Clermont Auvergne INP, CNRS, Institut Pascal, 63000 Clermont-Ferrand, France; salah_eddine.ouldboukhitine@uca.fr (S.-E.O.); christophe.vial@uca.fr (C.V.); joseph.gril@uca.fr (J.G.); rostand.moutou_pitti@uca.fr (R.M.P.)
2 Dagard Company, 23600 Boussac, France; nlabonne@dagard.com
3 Université Clermont Auvergne, INRAE, PIAF, 63000 Clermont-Ferrand, France
4 CENAREST, IRT, Libreville BP 14070, Gabon
5 MINES Paris, PSL Research University, PERSEE—Center for Processes, Renewable Energies and Energy Systems, 06904 Sophia Antipolis, France
6 California State Polytechnic University, Humboldt, School of Engineering, Arcata, CA 95521, USA
* Correspondence: yi_hien.chin@uca.fr (Y.H.C.); pascal.biwole@humboldt.edu (P.B.)

Abstract

Sustainable construction requires bio-based insulation materials that achieve low thermal conductivity without compromising mechanical performance. Poplar wood, which is locally abundant in France, serves as an effective carbon sink and represents a promising resource. While recent research has explored bulk wood delignification, the characterization of such modified materials remains insufficient for practical implementation. In this work, we report the development of gradient-delignified poplar wood through partial delignification using alcoholysis and sodium chlorite bleaching. This process produced a hybrid structure with delignified outer layers and a lignified core. Microscopic analyses revealed that lignin removal led to cell wall swelling and the formation of nano-scale pores. Compared to native poplar, the modified material showed lower transverse thermal conductivity (0.057 $W \cdot m^{-1} \cdot K^{-1}$), higher specific heat capacity (1.4 $kJ \cdot K^{-1} \cdot kg^{-1}$ at 20 °C), increased hygroscopicity, and reduced longitudinal compressive strength (15.9 MPa). The retention of the lignified core preserved dimensional stability and load-bearing capacity, thereby overcoming the limitations of complete delignification. In contrast to synthetic foams or mineral wools, these findings demonstrate that partial delignification can produce anisotropic wood-based insulation materials that combine thermal efficiency, mechanical stability, and biodegradability. This work highlights the potential of wood modification nanotechnology to reduce the carbon footprint of building materials.

Keywords: bio-based material; characterization; delignification; poplar; thermal insulation; wood nanotechnology

check for updates

Academic Editor: Przemysław Brzyski

Received: 25 August 2025
Revised: 3 October 2025
Accepted: 9 October 2025
Published: 20 October 2025

Citation: Chin, Y.H.; Ouldboukhitine, S.-E.; Vial, C.; Gril, J.; Moutou Pitti, R.; Labonne, N.; Biwole, P. Gradient-Delignified Wood as a Sustainable Anisotropic Insulation Material. *Energies* **2025**, *18*, 5519. https://doi.org/10.3390/en18205519

Copyright: © 2025 by the authors. Licensee MDPI, Basel, Switzerland. This article is an open access article distributed under the terms and conditions of the Creative Commons Attribution (CC BY) license (https://creativecommons.org/licenses/by/4.0/).

1. Introduction

To achieve the Sustainable Development Goals by reducing CO_2 and greenhouse gas emissions, it is necessary to substitute non-renewable materials with bio-based alternatives of low embodied energy [1]. Buildings alone account for 36% of the global energy load, which is related mainly to heating and cooling demands, making the development of a green, low-carbon, bio-based insulation material a priority [1]. Today's commercial market

for thermal insulation and sound absorption materials is dominated by synthetic porous structures produced from petroleum-based polymers, such as polyurethane foams and expanded/extruded polystyrene foams, and rock- and slag-based fibers such as mineral wools and glass wools [2]. While these materials are low-cost and effective insulators, they have significant environmental drawbacks. The extraction and synthesis processes of these materials have a high carbon footprint as they rely on non-renewable resources and generate pollutants. Schulte et al. reported through life cycle assessment studies that non-renewable insulation materials perform worst across most environmental impact categories [3]. Additionally, their disposal can cause environmental issues, resulting in a contradiction between their thermal efficiency and their environmental impact. Bio-based insulating products have therefore emerged as alternatives. Plant-derived materials retain carbon rather than emitting it, thereby contributing to a reduction in the overall carbon footprint [4]. However, they also present challenges such as susceptibility to fire, moisture attack, biological degradation (fungi, insects), and mechanical weaknesses. There is often a trade-off between the mechanical strength and thermal insulation properties of materials [5]. Wood appears to combine excellent mechanical characteristics and thermal insulating potential. For example, poplar wood (*Populus* spp.) with an average density of 450 $kg \cdot m^{-3}$ has been reported in the literature to exhibit a compressive strength of 35 MPa and a thermal conductivity of 0.16 $W \cdot m^{-1} \cdot K^{-1}$ [6]. The thermal conductivities of wood in the radial and tangential directions are nearly identical, whereas the conductivity along the grain has been reported to be higher than that across the grain by a factor of 1.5–2.8 [7]. The anisotropy of wood allows heat to dissipate along the direction of the grain.

Recent advances in wood modification nanotechnology, particularly delignification treatment, have opened new opportunities to enhance the existing beneficial characteristics of wood while improving its properties for novel applications. Delignification methods, which originate from lignocellulosic feedstock pulping and bleaching techniques, are used to improve the separation of carbohydrate components and to increase the yield of sugar and energy during combustion [8,9]. The idea of extracting cellulosic substances was further developed after the discovery of cellulose nanofibrils by Yano et al. [10]. Later, the top-down method was developed to treat wood without destroying the natural alignment of cellulose nanofibrils. A. Kumar et al. [11], Terzopoulou et al. [12], and J. Li et al. [13] reviewed experiments performed on wood delignification and the respective engineered wood. They concluded that delignification preserves the aligned cellulose structure while enabling tunable material properties, with potential applications in transparent wood, structural composites, biodegradable packaging, energy devices, and thermal management.

By creating nanopores through delignification, the thermal conductivity of wood has been reported to be significantly reduced [14,15]. Delignification creates voids in place of lignin and hemicelluloses, allowing their replacement with air of lower thermal conductivity or with other materials. However, excessive delignification can compromise mechanical integrity, requiring careful control of porosity, thickness, and treatment conditions to balance performance and structural stability. After the partial or complete removal of lignin and hemicelluloses, the treated wood is referred to as "delignified wood", "nanowood", "insulwood", "wood aerogel", "wood xerogel", "colorless wood", "cellulose scaffolds" or "white wood" [2,5,8,15–22]. Studies have reported its excellent thermal insulation properties, especially in the transverse direction. Delignified wood was shown to have a lower transverse thermal conductivity (0.032–0.051 $W \cdot m^{-1} \cdot K^{-1}$) than natural wood (0.065–0.156 $W \cdot m^{-1} \cdot K^{-1}$).

The lack of sufficient information and experimental studies on the use of delignified wood as a thermal insulator in large-scale applications drives this research. The hypothesis is that enhancing the porosity of the cell wall structure through delignification treatment

can reduce the density and thermal conductivity. While most existing delignification studies focus on complete lignin removal, our work demonstrates the advantages of partial delignification. Herein, we present the development and characterization of gradient-delignified poplar wood, a bio-based material that combines reduced thermal conductivity with structural stability. Unlike fully delignified materials, our gradient approach retains a lignified core that maintains load-bearing capacity while creating nanoporous delignified surfaces that lower the thermal conductivity. Through microscopic and macroscopic characterization, this study aims to verify the potential of such modified wood as a building material. Our findings fill a critical knowledge gap by providing, for the first time, a comprehensive thermal, hygric, and mechanical characterization of gradient-delignified wood. These properties were assessed using 100 cm^3 wood boards, which include both earlywood and latewood annual rings, representing the bulk wood structure and indicating the potential scalability of the material. For building-scale applications, larger treatment pilots or the assembly of multiple pieces would be required. The gradient-delignified wood offers a renewable alternative to synthetic foams, with the added benefits of carbon storage and reduced environmental footprint.

2. Materials and Methods

2.1. Materials

French poplar (*Populus* spp.) wood boards were purchased from Chagnon Carpentry (Boussac, France). They were cut into sections of 100 mm by 10 mm in the transverse plane and then longitudinally cut to 100 mm along the grain. Larger wood boards ($100 \times 100 \times 10$ mm^3) were used to prepare gradient-delignified wood, and small wood blocks ($10 \times 10 \times 10$ mm^3) were used to prepare completely delignified wood to characterize the properties of lignin-free wood. For comparison, stone wool and polyisocyanurate (PIR) foam, provided by Dagard (Purever Industries, Boussac, France), were used in the thermal and hygric characterizations. The chemical reagents used for wood delignification were purchased from Sigma-Aldrich (Darmstadt, Germany).

2.2. Wood Delignification Technique

Organosolv pulping via alcoholysis treatment with ethylene glycol has been reported to produce lignin-free wood after sodium chlorite bleaching [19,23]. The completely lignin-free wood was prepared using small wood blocks as described in the previous work [24]. For gradient-delignified wood, large wood boards were treated in a covered beaker attached to a condenser, and the temperature was monitored with a temperature probe connected to a hotplate stirrer. For one treatment procedure, a total of 750 mL of stock solution consisting of ethylene glycol, water, and 97% H_2SO_4 at a mass ratio of 99:0.5:0.5 was prepared for two wood boards. The wood boards were first impregnated in the solvent under vacuum for 90 min, and then heated in a covered beaker placed on a hotplate at 140 °C for 4 h. After the alcoholysis treatment, the excess reactants were removed from the samples by a washing procedure. Next, the wood was subjected to $NaClO_2$ bleaching at 70 °C for 8 h. The bleaching solution was prepared by dissolving 8 g of $NaClO_2$ powder in 1200 mL of water, and 1.6 mL of acetic acid was added. Every hour, an additional 8 g of $NaClO_2$ and 1.6 mL of acetic acid were added to the solution. Upon completion of the wood modification processes, the samples were rinsed thoroughly to remove the dissolved lignin and the excess reactants. The samples were first frozen in liquid nitrogen for 15 min, then freeze-dried at −95 °C and 13 hPa in the Heto PowerDry PL6000 freeze-dryer (Thermo Fisher Scientific, Waltham, MA, USA) located at the Institut Pascal (Université Clermont Auvergne, France) for 3 days.

The treatment of wood boards resulted in partial delignification, creating a composite material with white delignified surfaces and brown lignified core (Figure 1). Due to the wood's hierarchical structure, with lumens, pits, and rays influencing delignifying solvent flow, the sharp boundary between delignified and intact regions suggests incomplete diffusion. This finding introduced "gradient-delignified wood", which balances the desired thermal insulating properties of wood with the hygric and mechanical properties.

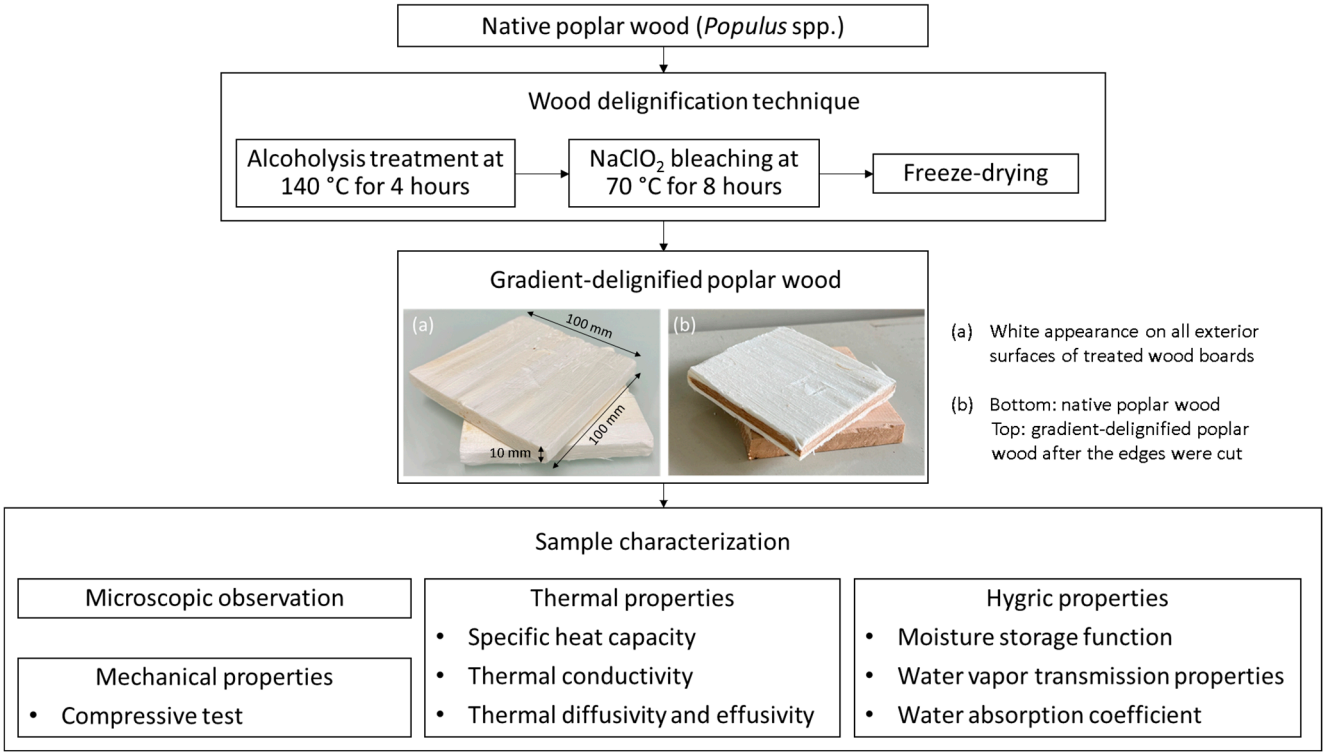


Figure 1. Flowchart of fabrication and characterization of gradient-delignified poplar wood made from 100 cm^3 wood boards in this work.

2.3. Sample Characterization

2.3.1. Microscopic Observation

For scanning electron microscopy (SEM) observations, the relevant surfaces of the native and gradient-delignified wood samples were prepared using a Leica RM2165 rotary microtome (Leica Microsystems, Wetzlar, Germany) to minimize damage to the wood structure. The samples were then mounted on stubs using adhesive carbon tabs and coated with platinum (Quorum Q150 TES, Quorum Technologies, Laughton, East Sussex, UK). Observations were carried out using a field emission scanning electron microscope Regulus 8230 (Hitachi, Tokyo, Japan) at 2 kV with a secondary electron detector at the Dunant site platform (CICS, Clermont-Ferrand, France).

2.3.2. Porosity

Porosity is a fraction of the volume of void over the total volume, between 0% and 100%, as defined in Equation (1). By assuming that the void space is filled with air, Equation (2) is often used to express the porosity of wood.

$$\text{Porosity} = \frac{V_v}{V_t} \times 100\% \quad (1)$$

where V_v [m^3] is the volume of void and V_t [m^3] is the total bulk volume of material.

$$\text{Porosity} = \left(1 - \frac{\rho_t}{\rho_*}\right) \times 100\% \quad (2)$$

where ρ_t [$kg \cdot m^{-3}$] is the bulk density (apparent density) of the wood and ρ_* [$kg \cdot m^{-3}$] is the density of the solid wood substance. The bulk density of the wood samples [$kg \cdot m^{-3}$] was calculated as the ratio of mass [kg] to apparent volume [m^3]. The density of the solid wood substance is an ideal physical value for a non-porous lignified cellulosic cell wall. It is very similar in all timbers (about 1500 $kg \cdot m^{-3}$) [25].

2.3.3. Thermal Property Characterization

1. Specific heat capacity

Specific heat capacities were measured using a Calvet BT2.15 calorimeter (Setaram, Caluire-et-Cuire, France) located in the Laboratory of Engineering Sciences for Environment (LaSIE—UMR 7356 La Rochelle Université—CNRS, La Rochelle, France). The calorimeter employs heat flux sensors that use Joule effect calibration and fully surround the sample during the measurement. This setup has a heat measurement efficiency of 95%. The temperature and enthalpy accuracies are ±0.5 °C and ±0.2%, respectively. The samples were precisely cut to fit the cylindrical sample holder of the calorimeter. The measurement protocol involved heating the sample at a constant rate of 0.1 °C.min^{-1} from −10 °C to 50 °C. An initial stabilization period of 3 h at −10 °C and a final stabilization period of 6 h at 50 °C were performed. The specific heat capacity was calculated via linear regression of the thermal capacity versus temperature data in the range from −5 °C to 45 °C.

The specific heat capacities of three different types of poplar wood (native poplar wood, delignified poplar wood, and gradient-delignified poplar wood) were determined. The delignified poplar wood sample used 1 cm^3 poplar wood blocks, which were completely delignified, whereas the gradient-delignified wood used a heterogeneous structure with varying degrees of delignification between the core and the surface.

2. Thermal conductivity

The thermal conductivity (k) of a material is defined as its ability to conduct heat. Under steady-state conditions, where the temperature distribution does not change over time, the thermal conductivity is governed by Fourier's law (Equation (3)). The higher the thermal conductivity is, the more efficiently heat flows through the material.

$$q = -k \nabla T \quad (3)$$

which the heat flux density q [$W \cdot m^{-2}$] is proportional to the temperature gradient ∇T [$K \cdot m^{-1}$] and the thermal conductivity k [$W \cdot m^{-1} \cdot K^{-1}$].

To compare the thermal conductivity of poplar wood before and after partial delignification, two measurement methods were employed: the hot wire method and the heat flow meter method.

The hot wire method is a transient technique performed using the FP2C conductivity meter (Neotim, Albi, France). This device can measure thermal conductivities ranging from 0.02 to 5 $W \cdot m^{-1} \cdot K^{-1}$ with an accuracy of 5%. We assume that the difference in the tangential and radial directions is negligible. Thus, wood is assumed to be an orthotropic material with two principal directions, the longitudinal direction and the transverse direction, by orienting the hot wire either along or across the grain direction. The "true" value of the thermal conductivity cannot be obtained, but it is possible to distinguish the longitudinal and transverse thermal conductivities [26,27]. It provides comparative data by applying a consistent methodology. For the hot wire method, two orientations relative to the wood

fibers were considered: parallel (∥) and perpendicular (⊥) to the fiber direction. When the hot wire is parallel to the fiber direction, the measurement reflects the transverse thermal conductivity. When perpendicular, the results consider both transverse and longitudinal conductivity.

Thermal conductivity measurements were also conducted at the laboratory in Dagard using a LaserComp FOX 314 thermal conductivity heat flow meter (TA Instruments, New Castle, DE, USA). It can measure thermal conductivities ranging from 0.005 to 0.35 $W \cdot m^{-1} \cdot K^{-1}$ with an accuracy of 1%. A temperature difference of 20 °C was applied across the plates, and each plate was equipped with a 100 mm × 100 mm heat flux transducer for the determination of thermal conductivity. To minimize edge effects, a polyisocyanurate foam frame was placed around the sample. The heat flow meter method only measures transverse thermal conductivity, limited by the wood sample format.

3. Thermal diffusivity and effusivity

The thermal diffusivity, α [$m^2 \cdot s^{-1}$], was measured using the hot ring probe (Neotim, Albi, France), which is capable of measuring the thermal diffusivity within the range of 0.1–4 $mm^2 \cdot s^{-1}$ with an accuracy of 10%. In addition, the thermal diffusivity was also calculated using Equation (4). The thermal effusivity, e [$J \cdot m^{-2} \cdot K^{-1} \cdot s^{-0.5}$], was measured using the hot surface probe (Neotim, Albi, France), which can measure thermal effusivity values ranging from 20 to 10,000 $J \cdot m^{-2} \cdot K^{-1} \cdot s^{-0.5}$ with an accuracy of 5%. Similarly, the thermal effusivity was also calculated, using Equation (5).

$$\alpha = \frac{k}{\rho \cdot C_p} \tag{4}$$

$$e = \sqrt{k \cdot \rho \cdot C_p} \tag{5}$$

where k, ρ, and C_p are the thermal conductivity [$W \cdot m^{-1} \cdot K^{-1}$], density [$kg \cdot m^{-3}$], and specific heat capacity [$J \cdot K^{-1} \cdot kg^{-1}$], respectively.

2.3.4. Hygric Property Characterization

1. Moisture storage function

The moisture storage function, also known as the vapor sorption capacity, is a property that describes the ability of a material to absorb and release water vapor from the surrounding environment. The isotherms were programmed using a dynamic vapor sorption (DVS) device that operates via a gravimetric method, the SPSx-1μ (ProUmid, Ulm, Germany) device located at the Laboratory of Engineering Sciences for Environment (LaSIE—UMR 7356 La Rochelle Université—CNRS, France). Measurements were conducted at a constant temperature of 25 °C, with the relative humidity increasing in steps of 15%, ranging from 0% to 90%, for both the adsorption and desorption phases. Due to the lightweight samples, the stability criterion between each step (dm/dt) was set at 0.003% over 120 min, which is close to the reproducibility limit of the weighing balance (5 μg), with manual deactivation when necessary. A preliminary drying phase was programmed in the device. The mass change kinetics during both drying and humidification were monitored by weighing the samples every 60 min. Each relative humidity took approximately two weeks to stabilize, with the entire analysis spanning over four months.

2. Water vapor transmission properties—Dry cup method

The dry cup method was selected to determine the water vapor resistance factor (μ) for four materials: stone wool, PIR foam, native poplar wood, and gradient-delignified poplar wood. The samples were prepared by cutting them into round shapes with a diameter of 6 cm, and their exact dimensions were measured. Silica gel was used as a desiccant to maintain the internal humidity between 0% and 2% RH, with a 15 mm air gap between

the silica gel and the sample. The dry cup was carefully sealed with silicone to ensure unidirectional moisture transfer. The test assemblies were placed in a HPP260 constant climate chamber (Memmert GmbH, Schwabach, Germany) set at 23 °C and 50% RH. The chamber provides constant temperature and RH conditions in the range from −10 °C to 70 °C and from 10% RH to 90% RH, with precisions ±0.1 °C and ±0.5%, respectively. The test assemblies were weighed every 4 h until the slope of the water vapor flux curve was constant. The data collected were used to determine the water vapor transmission properties according to NF EN ISO 12572 and NF EN ISO 12086 [28,29].

3. Water absorption coefficient by partial immersion

Liquid transport properties determine how quickly a material can absorb, distribute, and release water, influencing its overall performance for specific applications. To understand water absorption kinetics, the water absorption coefficient (A_w) is used to quantify the rate of water absorption in a material by the partial immersion method, as defined in NF EN ISO 15148 [30].

To determine the water absorption coefficient (A_w) for stone wool, PIR foam, native poplar wood, and gradient-delignified poplar wood, samples were cut into squares with 75 mm sides. The sides of each sample were sealed with silicone and dried at room temperature until they reached a constant mass. The samples were then partially immersed in water, with 3 mm of the thickness submerged on one face. After 5 min, the samples were removed from the water, and any excess surface moisture was wiped away with a damp cloth before weighing. This procedure of immersion, removal, surface drying, and weighing was repeated at increasing time intervals. The mass of water absorbed per unit area is plotted against the square root of time, with the slope of the initial linear portion of this curve representing A_w [kg·m^{-2}·s$^{-0.5}$] (Equation (6)).

$$\mathrm{A}_w = \frac{\Delta m}{S\sqrt{t}} \tag{6}$$

where Δm [kg] is the change in mass, S [m^2] is the immersed surface area, and t [s] is the time. The slope of the plot of $\Delta m/S$ against $\sqrt{t}$ was used to determine the coefficient A_w.

The coefficient A_w can be used to determine the liquid transport coefficient for suction (D_{ws}), which is the rate of moisture flow through a material under a unit difference in moisture concentration. D_{ws} [m^2·s^{-1}] is calculated with the water absorption coefficient and the moisture storage function using Equation (7).

$$D_{ws}(w) = 3.8 \cdot (A/w_f)^2 \cdot 1000^{(w/wf)-1} \tag{7}$$

where w [kg·m^{-3}] is the moisture content and w_f [kg·m^{-3}] is the free water saturation.

2.3.5. Mechanical Property Characterization

To evaluate the potential of gradient-delignified wood as a thermal insulating material, compressive tests were conducted following the NF EN 826 standard [31]. These tests were performed using a universal testing machine (Dagard, Boussac, France) equipped with a 10 kN load cell at a crosshead speed of 1 mm.min^{-1}. The samples were carefully cut from larger wood boards with approximate side lengths of 10 mm. The samples were conditioned in an ambient environment (20 °C, ~60% RH). Before testing, the samples were weighed, and their exact dimensions were measured using a digital caliper for the following calculations of stress and strain. Three samples were prepared for each directional orientation (longitudinal, radial, and tangential) to ensure an average evaluation of the compressive properties. Stress–strain (σ-ε) curves were plotted from the recorded force and displacement data.

3. Results and Discussion

3.1. Microscopic Observations

SEM images can provide visual analysis of the microstructural differences between native poplar wood and gradient-delignified poplar wood. The images presented in Figure 2 illustrate how the delignification process progressively alters the wood architecture, particularly affecting the interconnectivity of wood fiber cells and overall porosity.

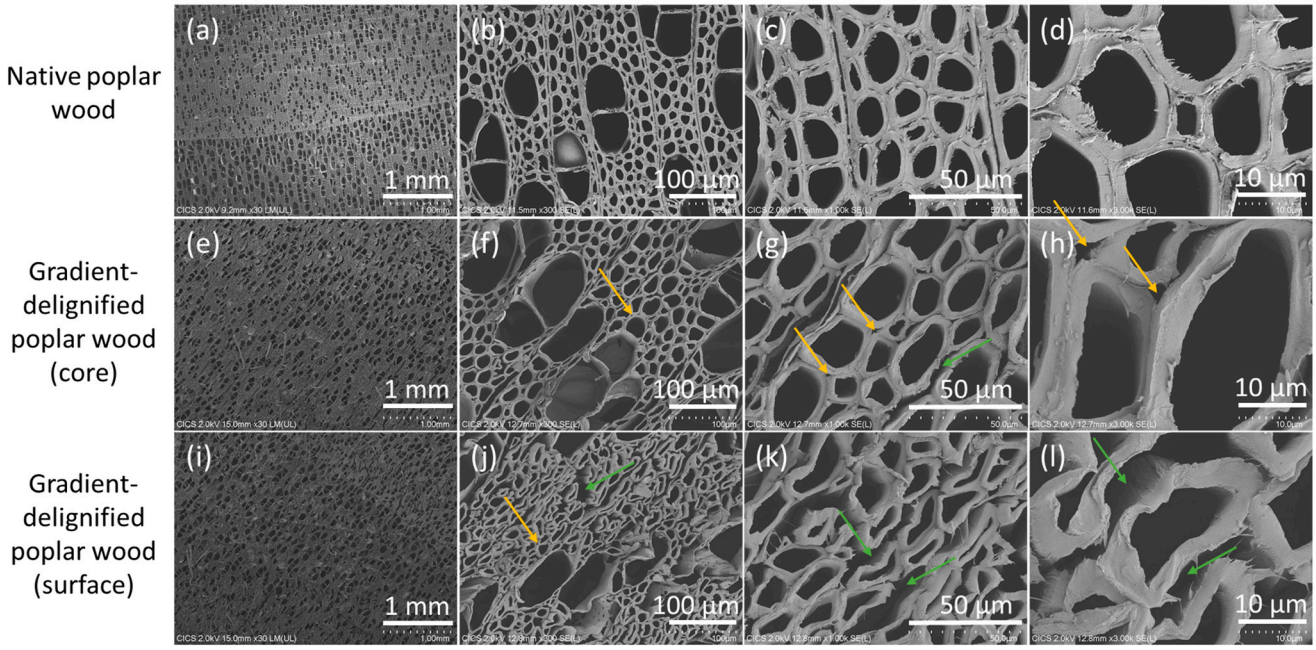


Figure 2. SEM images of the (**a**–**d**) native poplar wood, (**e**–**h**) core, and (**i**–**l**) surface of gradient-delignified poplar wood. Yellow arrows indicate the delignified cell wall corners, and green arrows indicate the cell wall separation.

SEM images in the literature revealed that the native hierarchical structure of wood is preserved at the microscale after delignification, with the overall honeycomb-like architecture remaining intact. In the nanostructure, the orientation of the cellulose fibrils was preserved along the cell axis [32,33]. Cellulose fibrils were reported to appear as small white dots on the surface, and the removal of lignin isolates these fibrils and creates spaces between them. The formation of new pores within the cell wall and cracks in the former lignin-rich cell corners explains the increase in porosity after delignification treatment [32]. Kurei et al. [34] carried out a detailed analysis of SEM images of Japanese cedar subjected to different treatments to reduce the content of wood components (polysaccharide or lignin). After the complete removal of lignin through a combination of alcoholysis and sodium chlorite bleaching treatment, the cell arrangement remained unchanged. However, the lack of lignin causes more significant transverse swelling due to the loss of adhesion force between wood cells. The complete delignification treatment was reported to remove the cell corner substances and round off the shape of the cells [34].

Figure 2a shows that the native poplar wood has a typical structure of diffuse-porous hardwood. The cell walls range from 1.46 to 3.78 µm thick and maintain a well-organized and tightly packed cellular arrangement. In the central region of the gradient-delignified wood (core), a slight alteration in the wood architecture was observed. Figure 2h shows the presence of small spaces at the cell wall corner, indicating the partial removal of non-cellulosic substances from the middle lamella. The overall structure remained largely similar to that of native wood. The cell wall thickness in this region ranges from 1.77 µm to 3.58 µm (Table 1), suggesting that incomplete lignin removal allows the preservation

of the core's structural integrity. In contrast, the peripheral region of gradient-delignified wood (surface), which was directly exposed to the delignifying solution, presented a more deformed cellular structure. Here, the cell wall thickness varies from 2.17 to 3.98 µm. Figure 2k shows significant deformation of the lumens and vessels, with a remarkable collapse of the wood fibers. This region exhibited more extensive or nearly complete lignin removal, resulting in wood cell isolation and more open spaces at the cell wall corner, further increasing the porosity of the wood. This increased porosity likely increased the water absorption capacity and reduced the thermal conductivity, making it suitable for insulation applications. However, these structural changes also compromised the mechanical performance of the wood due to the loss of lignin, which serves as a binding component for the strength and rigidity of the wood. By combining the properties of the central and peripheral regions of the gradient-delignified wood, both the thermal and mechanical properties can reach equilibrium.

Table 1. Thickness of wood cell walls measured on SEM images of native and gradient-delignified poplar wood.

Type of Poplar Wood	Cell Wall Thickness [µm]
Native	1.46–3.78
Gradient-delignified (core)	1.77–3.58
Gradient-delignified (surface)	2.17–3.98

The partial delignification process in bulk wood resulted in a gradient of non-cellulosic substances removal, with the delignification efficiency increasing from the core to the surface of the wood. This gradient led to an increase in porosity and eventual deformation of the lumen, particularly toward the outer regions. Despite the loss of substances and associated mass loss, the cell walls in gradient-delignified wood are thicker than those in native wood (Figure 3). This observation suggests that the wood cell walls underwent swelling during the delignification process, likely due to the absorption of the delignifying solution and the subsequent removal of lignin, which created nano-scale pores within the cell walls. The increased porosity and thicker cell walls in gradient-delignified wood, as evident in the SEM images, suggest that this material could be a promising option for thermal insulation applications.

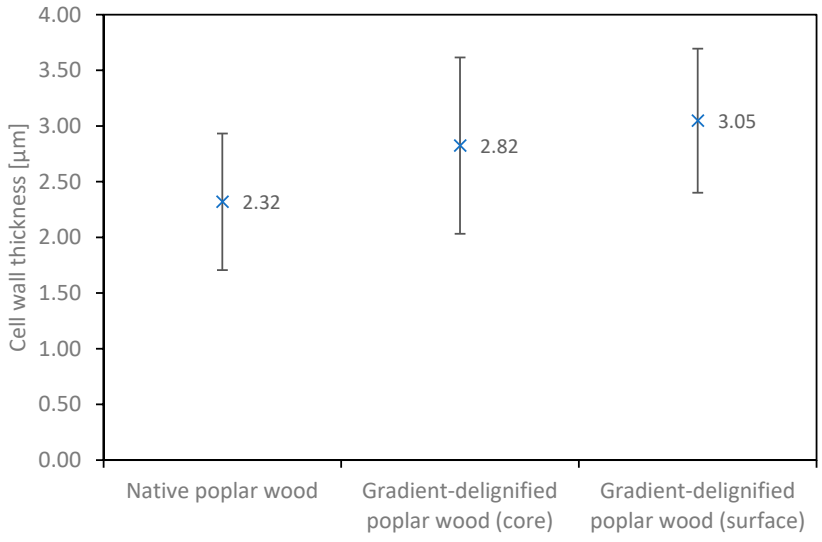


Figure 3. Cell wall thickness of native and gradient-delignified poplar wood measured on SEM images (mean cell wall thickness [µm] ± standard deviation).

3.2. Thermal Properties

3.2.1. Specific Heat Capacity

The specific heat capacity (C_p) of a material allows us to understand its thermal behavior, particularly in applications related to insulation. The specific heat capacity determines the amount of heat energy required to increase the temperature of a material, which directly influences how quickly it heats up and cools down in response to environmental changes. This property is important for building materials where thermal performance and energy efficiency are key considerations. The specific heat capacity of wood is generally independent of density or species [7], but it varies with temperature, moisture content, and state of matter. Experimentally, the average specific heat capacity of wood has been determined to be approximately 1.356 $kJ \cdot K^{-1} \cdot kg^{-1}$. However, each wood component has different specific heat capacities, for example, 1.549 $kJ \cdot K^{-1} \cdot kg^{-1}$ for cellulose and 0.67 $kJ \cdot K^{-1} \cdot kg^{-1}$ for charcoal [25]. Liquid water has one of the highest specific heat capacities among common substances, approximately 4.184 $kJ \cdot K^{-1} \cdot kg^{-1}$ at 20 °C. Hence, moist wood has a higher heat capacity than dry wood. Above the fiber saturation point, the additional moisture significantly contributes to the heat capacity of wood [7]. Compared with native wood, delignified wood, which has been treated to remove non-cellulosic substances, possesses different thermal properties.

Across the temperature range examined, the specific heat capacity of all the wood samples increased with temperature (Figure 4). This behavior is common for most materials, as more energy input is generally required for further temperature increases, suggesting that the materials become less efficient at storing thermal energy at lower temperatures. Importantly, the temperature variation has a non-negligible effect on the heat capacity of a material.

Among the three types of poplar wood, delignified poplar wood presented the highest specific heat capacity across the entire temperature range. This finding indicates that the removal of lignin significantly improves the ability of a material to store thermal energy. This observation aligns with previous findings by Garemark et al., who also reported that delignification can lead to increased specific heat capacity [17]. By applying the rule of mixtures without considering the latent heat of phase change, the specific heat capacity of delignified wood with a high relative cellulose content is close to the value of cellulose. Native poplar wood presented the lowest specific heat capacity, which implied that it heats up and cools down more quickly than the delignified samples do. The low specific heat capacity values can be attributed to the presence of lignin, which has a lower specific heat capacity than cellulose and hemicelluloses. Gradient-delignified poplar wood, with intermediate specific heat capacity values, demonstrated a clear correlation between the degree of lignin removal and the increase in specific heat capacity. The partial delignification process, which leaves the wood with a heterogeneous structure, results in equivalent thermal properties that fall between those of fully delignified and native wood.

The data presented in Figure 4 are useful for modeling heat transfer through walls when evaluating the thermal performance of buildings. The higher specific heat capacity of treated poplar wood indicates that it can absorb and store more heat, leading to slower temperature fluctuations and increased thermal inertia. It offers a longer thermal lag, meaning that it takes longer to reach equilibrium with the surrounding temperature. This property is beneficial in colder climates, where the thermal mass can regulate the indoor temperature more efficiently and reduce energy consumption by minimizing the need for an active heating system. In contrast, conventional insulating materials such as polystyrene, which typically have a specific heat capacity of approximately 1.2 $kJ \cdot K^{-1} \cdot kg^{-1}$, contribute less to the overall thermal mass of a building due to their low density [35,36]. Native poplar wood already has a higher specific heat capacity than synthetic insulation materials do, making it an ideal building material when thermal insulation, thermal mass, and ecology

are desirable. The increased heat capacity after wood delignification further enhances its potential as a sustainable and efficient building material, offering the dual benefits of improved thermal inertia and reduced heat propagation over time. However, in warmer climates, the same effect can prolong elevated indoor temperatures, potentially increasing the need for cooling. Therefore, the application of such materials should be carefully evaluated depending on the building's climatic design.

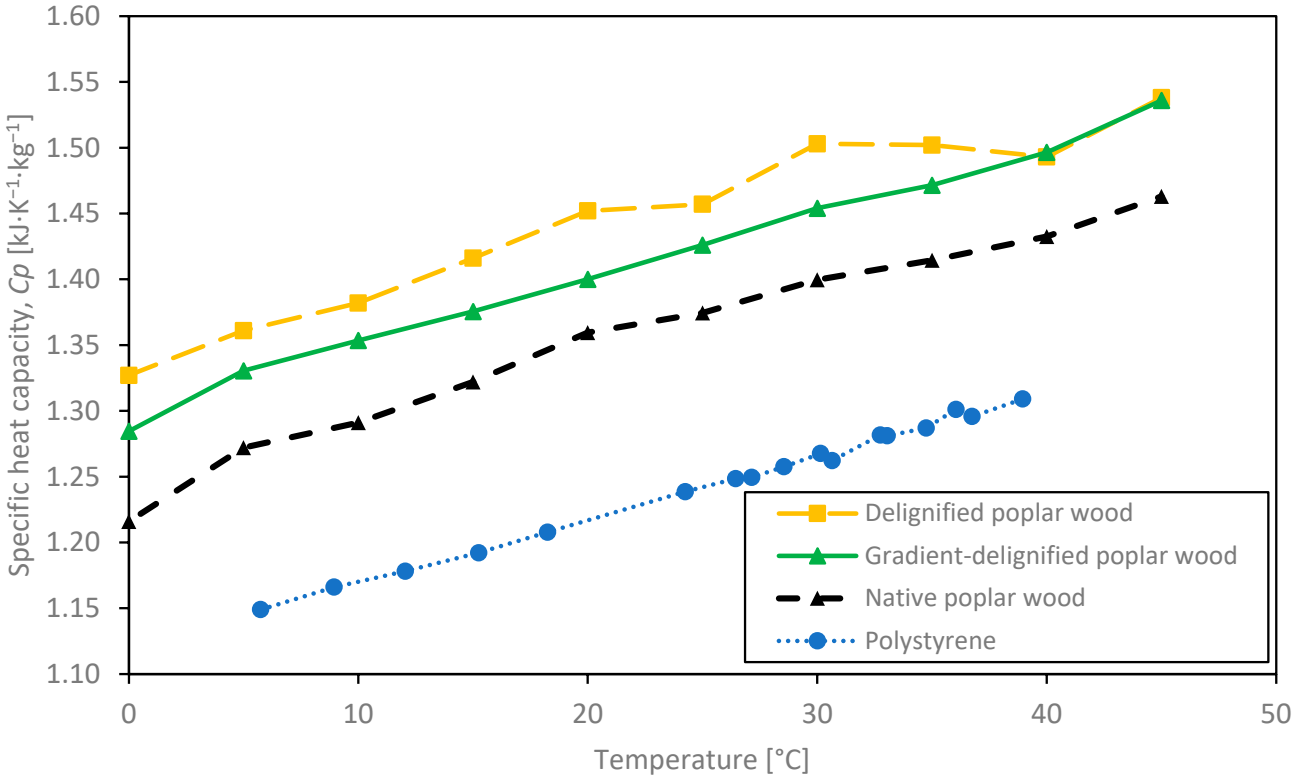


Figure 4. Specific heat capacity of different types of poplar wood across a temperature range from −5 °C to 45 °C, compared with the reported values of polystyrene [37].

3.2.2. Thermal Conductivity

In the design and selection of building materials, the thermal conductivity of materials is the most important for energy savings and thermal insulation. By selecting materials with low thermal conductivity, the energy efficiency of buildings can be significantly improved, leading to reduced heating and cooling costs [14]. In homogeneous materials such as metals, heat is transferred evenly in all directions, which is known as isotropy. However, the thermal conductivity of wood is not uniform in all directions because of its anisotropic nature. The properties of anisotropic materials vary depending on the direction in which they are measured. Wood's anisotropy is due to its cellular structure, which includes radial, tangential, and longitudinal orientations and the development of earlywood and latewood for each annual ring [38]. Its thermal conductivity is lower in the direction perpendicular to the fiber axis because the heat path is interrupted by air-filled lumens. In contrast, the thermal conductivity of wood is greater along the grain (longitudinal direction parallel to the fiber axis). Furthermore, the thermal conductivity of wood is influenced by density, the presence of extractives and defects, and especially the moisture content [25].

The thermal conductivity measurements of native poplar wood and gradient-delignified poplar wood using the hot wire method are shown in Figure 5. The results indicated a lower thermal conductivity when the wire was placed parallel to the fibers. This value, which represents the equivalent thermal conductivity of the radial and tangential

directions of the wood, aligns with the expectation that heat transfer is less efficient across the grain. After partial delignification, the thermal conductivity decreased in both orientations. This reduction was attributed to the removal of lignin, which increased porosity and reduced wood density. The newly formed pore spaces disrupted heat conduction pathways, leading to lower thermal conductivity. The higher standard deviation observed for gradient-delignified wood is attributed to the heterogeneity of the material. Different regions may be more or less delignified, leading to variability in local thermal properties.

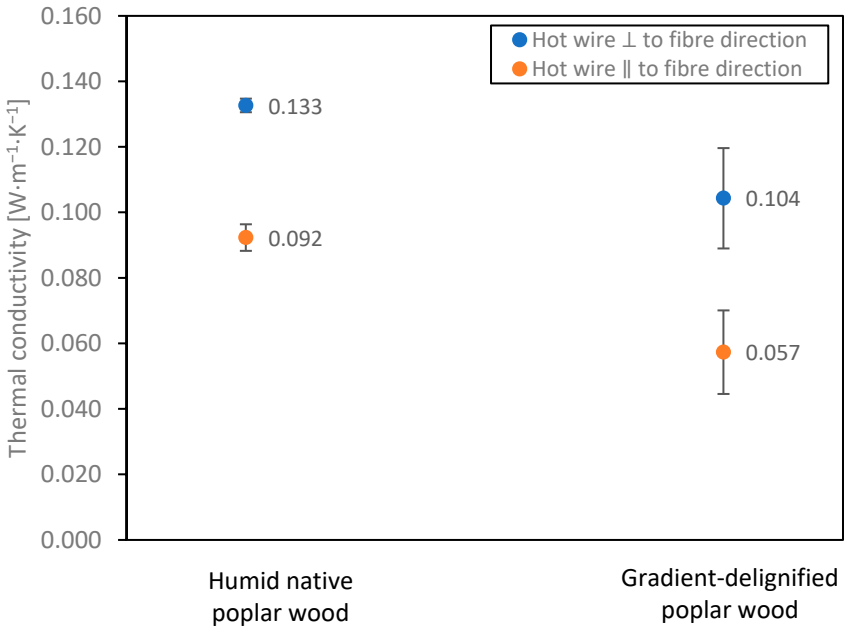


Figure 5. Thermal conductivities of native and gradient-delignified poplar wood measured by the hot wire method (thermal conductivity [$W \cdot m^{-1} \cdot K^{-1}$] ± standard deviation).

Figure 6 presents the relationship between the density and transverse thermal conductivity of different materials: humid and dry native poplar, gradient-delignified poplar, stone wool, and PIR insulation. The data measured using a heat flow meter confirmed that the moisture content significantly influences the thermal conductivity of wood. Humid native poplar wood has the highest transverse thermal conductivity (0.091 $W \cdot m^{-1} \cdot K^{-1}$) because water has a higher conductivity than air. Dry native poplar wood has a reduced thermal conductivity (0.079 $W \cdot m^{-1} \cdot K^{-1}$), highlighting the importance of moisture control for better insulating properties. The use of gradient-delignified poplar wood further reduces the transverse thermal conductivity to 0.057 $W \cdot m^{-1} \cdot K^{-1}$, primarily due to increased porosity, which increases from 72% to 82% in native wood. This increased porosity allows more air to be captured within the structure, improving its insulation properties. However, compared with conventional insulators such as stone wool and PIR, gradient-delignified poplar does not meet the insulating effectiveness requirements ($\leq$0.042 $W \cdot m^{-1} \cdot K^{-1}$).

The agreement between the heat flow meter and the hot wire (parallel to the fiber direction) confirmed the reliability of measuring the transverse thermal conductivity in this orientation. Both techniques consistently demonstrated a reduction in thermal conductivity after delignification. Figure 7 shows the decrease in transverse and longitudinal thermal conductivity as a function of wood density, in comparison with literature data. Anisotropy was observed by the higher values measured in the longitudinal direction due to the axial fiber orientation. The gradient-delignified wood developed in this work (yellow empty markers) presents a balanced combination of thermal conductivity and density, positioned between natural and fully delignified wood. Overall, these results demonstrated that

delignification treatment can improve the thermal insulating ability of wood. To meet the requirements of thermal resistance for applications, increasing the material's thickness might be necessary. Additionally, maintaining a low moisture content in the material is important, as increased humidity directly increases the thermal conductivity, thus reducing the insulation efficiency. This highlights the need to understand the hygric properties of wood-based insulation materials.

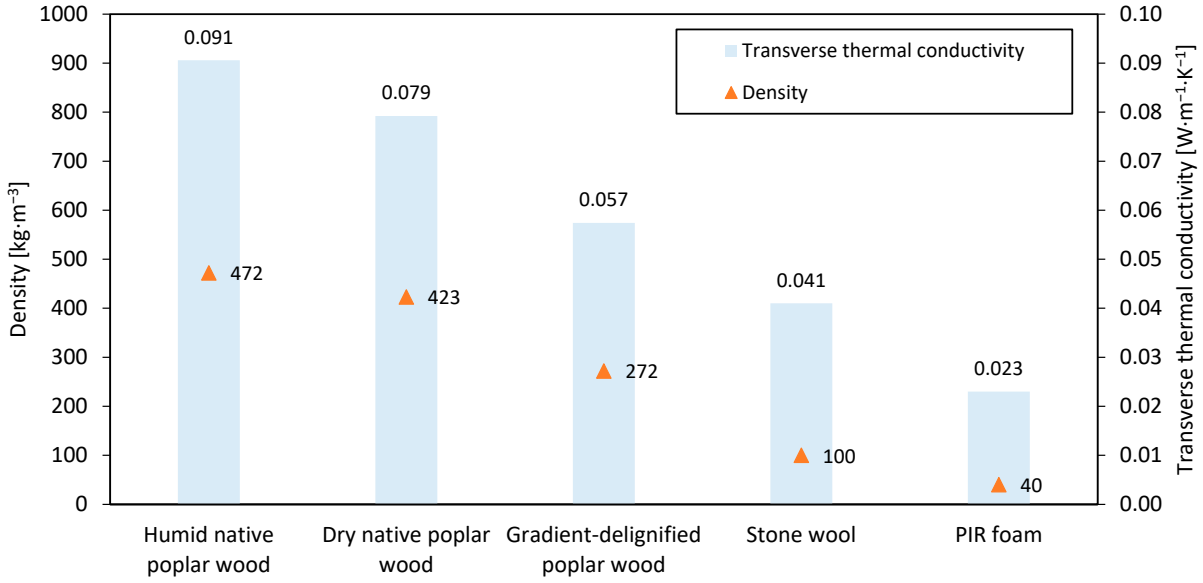


Figure 6. Thermal conductivities of native, gradient-delignified poplar, stone wool, and PIR samples measured with a heat flow meter, along with their densities.

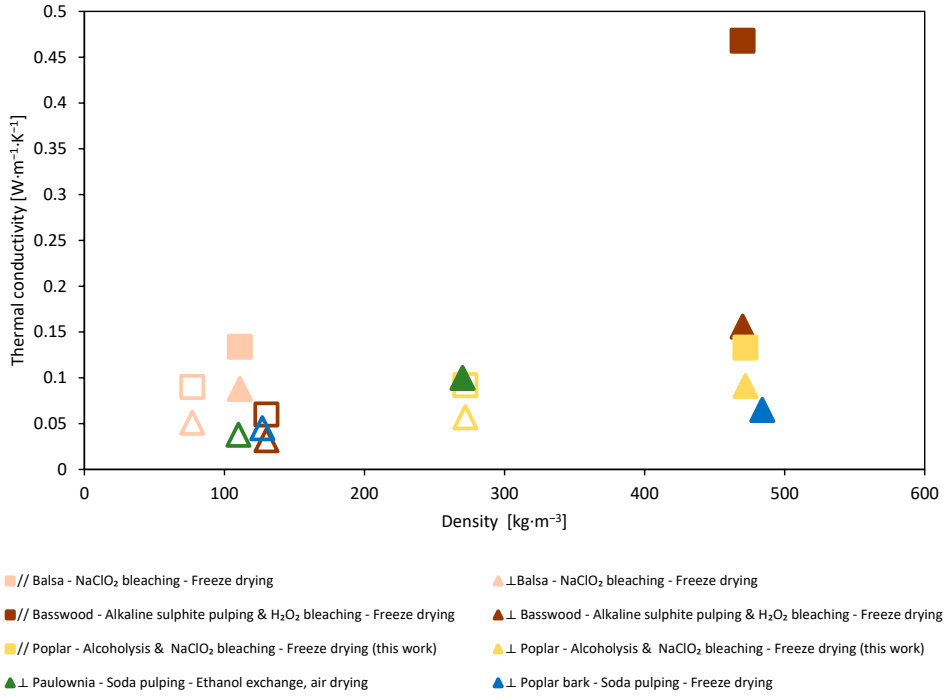


Figure 7. Reduction in thermal conductivity of wood after delignification treatment, compared with literature data [2,15,17,39,40]. Squares (//) represent longitudinal thermal conductivity, triangles (⊥) represent transverse thermal conductivity. Filled markers indicate natural wood before treatment, while empty markers indicate values after treatment. Legends specify wood species, treatment method, and drying method.

3.2.3. Heat Diffusivity and Effusivity

With the specific heat capacity and thermal conductivity data from the previous sections, the thermal effusivity and diffusivity of native and gradient-delignified poplar wood can be determined. These calculated values were then compared with direct measurements obtained using a hot ring probe and a hot surface probe. Table 2 presents the thermal effusivity and diffusivity for both native and gradient-delignified poplar wood, which were derived from their respective densities, specific heat capacities, and thermal conductivities.

Table 2. Thermal effusivity and diffusivity of native and gradient-delignified poplar wood calculated by equations via density, specific heat capacity, and transverse thermal conductivity measured by the heat flow meter method.

Properties	Native Poplar Wood	Gradient-Delignified Poplar Wood
Density, ρ [$kg \cdot m^{-3}$]	423	272
Porosity [%]	71.8	81.9
Specific heat capacity at 20 °C, C_p [$kJ \cdot K^{-1} \cdot kg^{-1}$]	1.36	1.40
Transverse thermal conductivity, *k* [$W \cdot m^{-1} \cdot K^{-1}$]	0.079	0.057
Transverse thermal effusivity, *e* [$J \cdot m^{-2} \cdot K^{-1} \cdot s^{-0.5}$]	213.18	147.32
Transverse thermal diffusivity, α [10^{-7} $m^2 \cdot s^{-1}$]	1.37	1.50

The thermal effusivity, which measures a material's ability to exchange heat with its environment, decreased from 213.18 $J \cdot m^{-2} \cdot K^{-1} \cdot s^{-0.5}$ in native poplar wood to 147.32 $J \cdot m^{-2} \cdot K^{-1} \cdot s^{-0.5}$ in gradient-delignified poplar wood. This reduction was primarily due to the lower density and thermal conductivity of the wood after treatment, despite its slightly higher specific heat capacity. The lower value of thermal effusivity suggests that gradient-delignified poplar wood feels less "cold" to the touch as it absorbs heat from its surroundings more slowly than native wood does.

The thermal diffusivity, which indicates the rate at which heat spreads through a material, increased slightly from 1.37×10^{-7} $m^2 \cdot s^{-1}$ in native poplar wood to 1.50×10^{-7} $m^2 \cdot s^{-1}$ in gradient-delignified poplar wood. This increase was attributed mainly to the lower density following delignification. This indicated that heat propagates faster through the gradient-delignified wood than through its native state. Garemark et al. also reported that the thermal diffusivity of balsa wood increases after delignification, from 4.7×10^{-7} $m^2 \cdot s^{-1}$ to 8.7×10^{-7} $m^2 \cdot s^{-1}$ in the axial direction and from 3.0×10^{-7} $m^2 \cdot s^{-1}$ to 5.0×10^{-7} $m^2 \cdot s^{-1}$ in the radial direction [17]. This increase suggests that the internal temperature of delignified wood can be adjusted more quickly in response to external heat sources.

The experimental measurements of thermal effusivity and diffusivity confirmed the observed trends after partial delignification, although they may not represent absolute values because of the anisotropic nature of wood. The coherence between the calculated and measured results strengthened the understanding that partial removal of non-cellulosic substances reduces the thermal conductivity and effusivity while increasing the thermal diffusivity (Figures 8 and 9). These findings, combined with data on specific heat capacity and thermal conductivity, provide valuable insight into how delignification alters the thermal performance of poplar wood, which can further be used to evaluate the feasibility of using gradient-delignified poplar wood as a thermal insulation material.

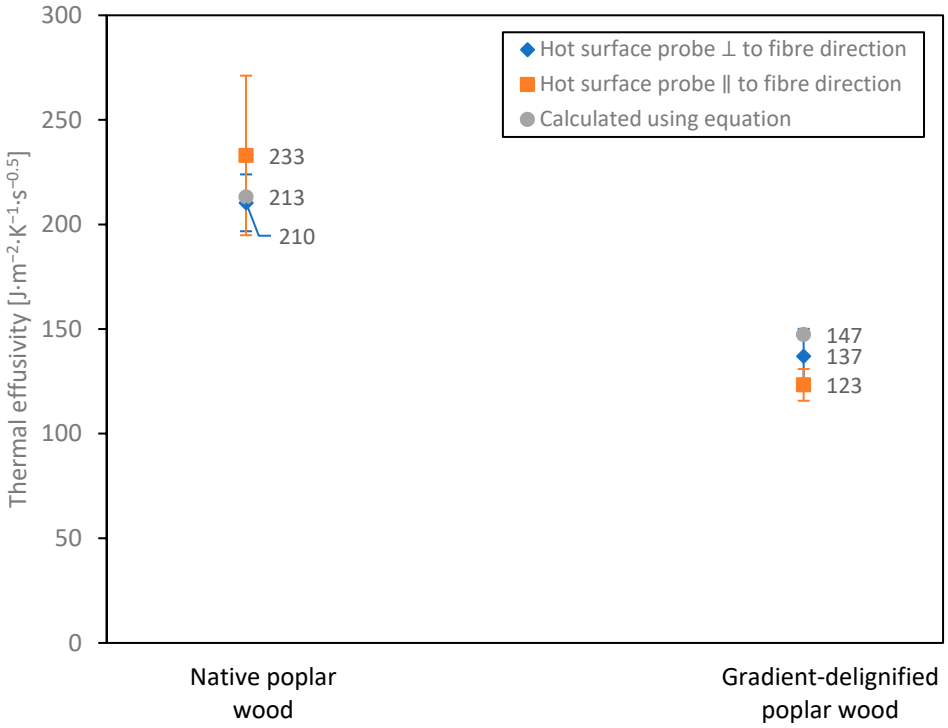


Figure 8. Thermal effusivity measured by a hot surface probe of native and gradient-delignified poplar wood (thermal effusivity [$J \cdot m^{-2} \cdot K^{-1} \cdot s^{-0.5}$] ± standard deviation).

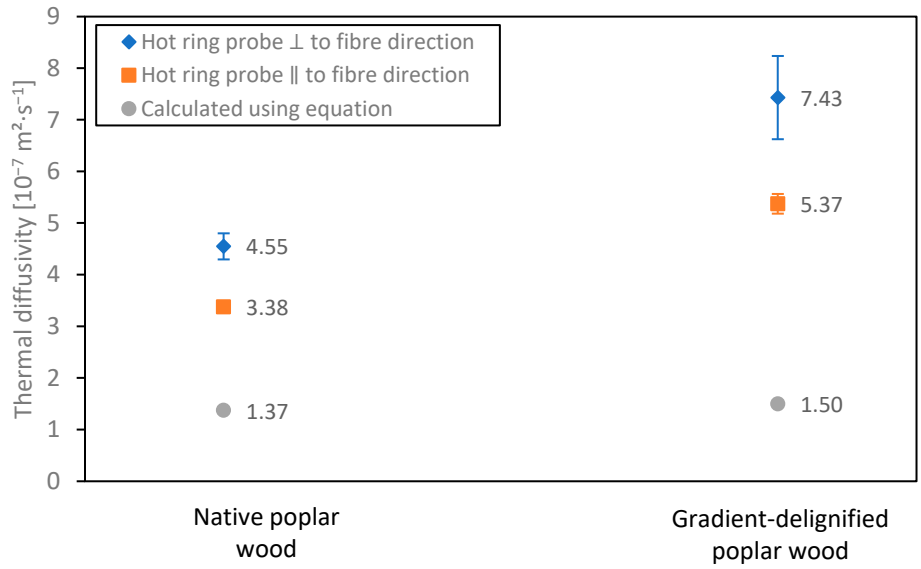


Figure 9. Thermal diffusivity measured by a hot ring probe of native and gradient-delignified poplar wood (thermal diffusivity [10^{-7} $m^2 \cdot s^{-1}$] ± standard deviation).

3.3. Hygric Properties

3.3.1. Moisture Storage Function

The moisture storage function is important for building materials, as it helps regulate indoor humidity levels to maintain a healthy indoor environment. Additionally, it allows the understanding of how materials behave in moist surroundings, which is useful for predicting dimensional variations due to relative humidity changes. These dimensional changes are linked to fluctuations in the water content of the material, making the study of moisture storage functions essential for the performance and durability of wood-based

products [4]. A wood will adsorb surrounding condensable vapors until its equilibrium moisture content is reached. The sorption isotherms for native poplar wood, delignified poplar wood, and gradient-delignified poplar wood are shown in Figure 10.

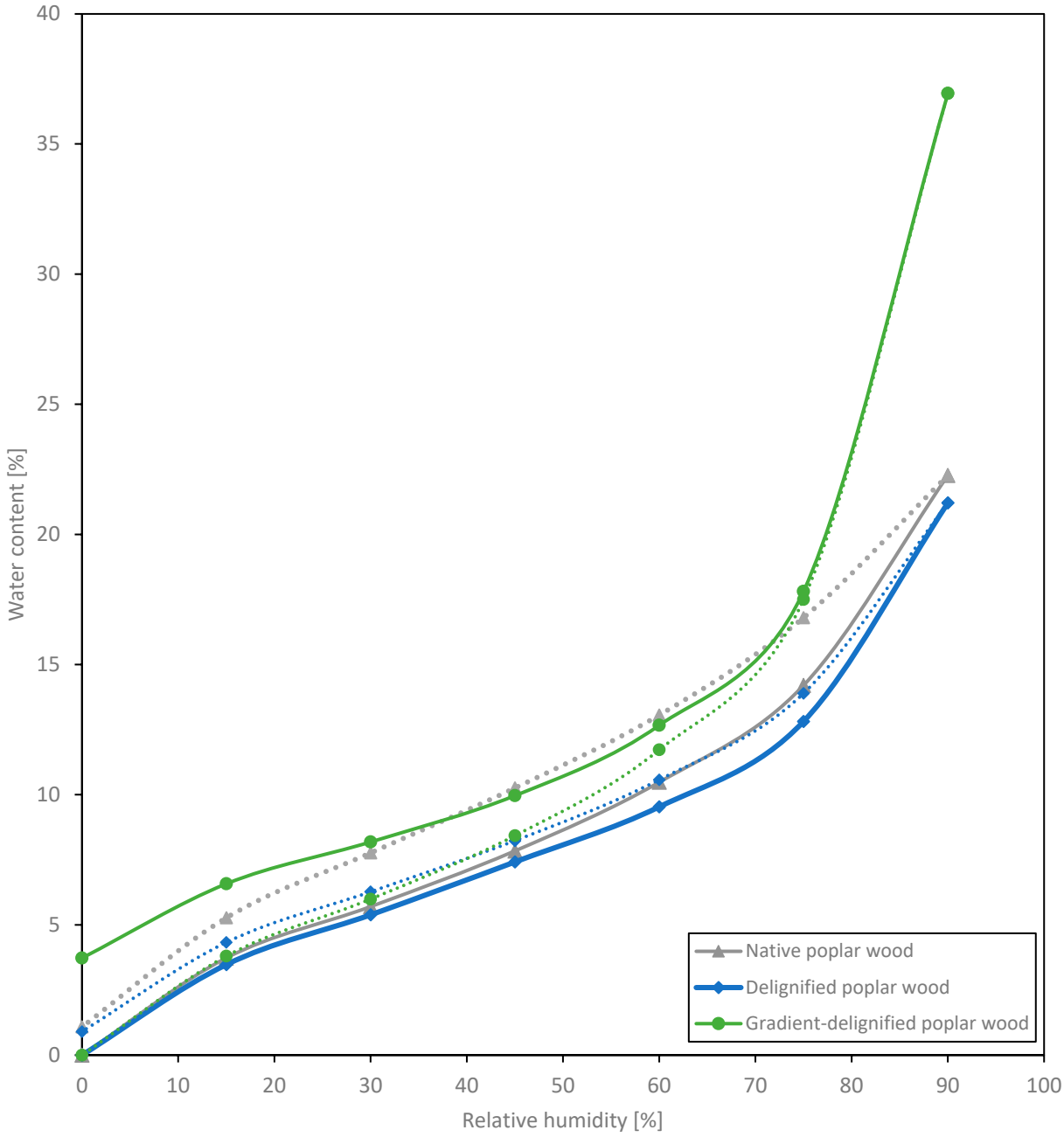


Figure 10. Sorption isotherms of native poplar wood, delignified poplar wood, and gradient-delignified poplar wood (solid line: adsorption; dotted line: desorption).

Delignification significantly altered the moisture sorption behavior of the wood. Lignin is a hydrophobic structural polymer that helps reduce the wood's sensitivity to moisture. When lignin is removed, the number of accessible hydroxyl (OH) groups in the wood cell wall increases and attracts more moisture. Grönquist et al. investigated sorption isotherms at different levels of delignification. Norway spruce cubes of 5 mm side length were treated with a mixture of hydrogen peroxide and acetic acid (H_2O_2/AA) at 80 °C for durations ranging from 15 to 360 min [41]. Without prior freeze-drying, the delignified wood was dried at 60 °C for 6 h at a partial water vapor pressure of $p/p_0 = 0$ under nitrogen flow

directly in the DVS instrument. The results indicated that gradient-delignified samples adsorbed more water than did native wood, but further delignification led to a decrease in adsorption capacity, likely due to the collapse of the wood cell wall structure after drying, as the supporting matrix of lignin was removed [41]. Montarina et al. [42] further modified delignified wood and investigated the effects of esterifying delignified wood with various anhydrides, such as maleic, itaconic, and succinic anhydrides. These esterification treatments were reported to reduce moisture uptake by introducing a bulking effect in wood cell walls, which decreases the chemical accessibility of water to limit hygroscopicity in transparent wood applications [42].

The sorption isotherms revealed how the water content in these materials varies with the surrounding relative humidity (RH). An IUPAC type II H3 pattern was identified, indicating that macropores with capillary condensation dominate the material's behavior. Both native and completely delignified poplar wood showed similar moisture absorption behaviors, with delignified wood having a lower moisture storage capacity. This phenomenon suggested that fully delignified wood is more susceptible to irreversible collapse, leading to a reduction in porosity during testing [41]. Water vapor diffused from the surface to the core through adsorption and capillary action in the pores. This movement, without saturating the entire sample, caused wetting and drying across the sample. Consequently, the collapse of wood cells occurs, but this phenomenon needs to be further verified using nitrogen sorption or SEM observations.

The gradient-delignified poplar wood presented a distinct pattern, with a relatively high water content across all RH levels. Especially at RH levels above 75%, the water content in gradient-delignified wood increased steeply, indicating a high sensitivity to humidity. This increased moisture absorption can be attributed to the material's composition. Hemicelluloses have been reported to have the highest sorptive capacity and contribute 37% to the total sorption of wood, followed by cellulose and lignin, which contribute 47% and 16%, respectively [25]. Delignified zones (white areas) are primarily composed of hydrophilic cellulose, which absorbs water more efficiently from the environment, whereas the remaining zones (brown areas) with remaining hemicelluloses and lignin store more moisture, contributing to the overall higher water content (Figure 11). In terms of sorption kinetics, the mass of the gradient-delignified samples increased immediately when the relative humidity changed, followed by a gradual decrease. Additional tests were conducted on these samples by placing them in environments of 15% and then 50% relative humidity. The same behavior was observed when the mass was measured every 60 min, suggesting that gradient-delignified wood underwent compositional changes when subjected to variations in ambient humidity.

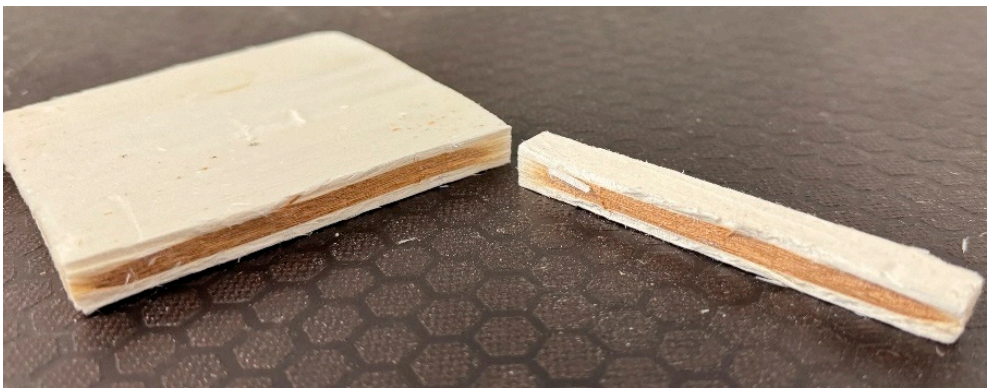


Figure 11. Image of gradient-delignified poplar wood comprising delignified (white color) and lignified (brown color) zones.

At high RH levels, gradient-delignified poplar wood can reach a water content of up to 35–40%, which is significantly higher than the 20–25% observed in native and fully delignified wood. This suggests that while gradient-delignified wood may be advantageous for moisture regulation in indoor environments, caution is necessary to avoid exceeding moisture levels that could promote mold growth. Additional treatment or protection might be needed. Below 75% RH, the differences among the wood samples remain minimal and are influenced mainly by sample size and wood orientation. At the end of the desorption stage, when the relative humidity reached 0%, gradient-delignified wood samples presented masses lower than their initial dry mass. This final mass is considered the sample's dry mass, and the water content is calculated relative to it, rather than assuming an initial water content of zero. The hypothesis is that residual chemical reagents in the wood gain moisture during the test, potentially reactivating and degrading some wood components. These newly discovered results demonstrated the impact of partial delignification on the moisture-handling properties of wood, where increased porosity and cellulose exposure on the surface led to increased water absorption.

Understanding the moisture storage function of a material is essential for evaluating its hygrothermal performance, particularly in building applications where the thermal conductivity is highly affected by the moisture content. Sorption isotherms allow better prediction of hygrothermal behavior at larger scales and identify the need for protective treatments or further modifications for suitable applications.

3.3.2. Water Vapor Transmission Properties

In the performance evaluation of bio-based materials in terms of thermal insulation and durability, the water vapor diffusion resistance factor (μ) is an important factor. This indicates how much the material is more resistant to diffusion than an air layer of the same thickness at the same temperature. A lower μ value indicates a material's higher permeability to water vapor, reflecting its hydrophilic nature. The results of the water vapor transmission properties of various materials, including stone wool, polyisocyanurate (PIR), native poplar wood, and gradient-delignified poplar wood, obtained from dry cup tests, are presented in Table 3.

Table 3. Water vapor transmission properties of various materials obtained from dry cup tests.

Water Vapor Transmission Properties	Stone Wool	PIR	Native Poplar Wood	Gradient-Delignified Poplar Wood
Water vapor permeance, W [10^{-10} kg·Pa^{-1}·m^{-2}·s^{-1}]	17.159	2.507	1.832	3.602
Corrected water vapor permeance (without air layer resistance), W_c [10^{-10} kg·Pa^{-1}·m^{-2}·s^{-1}]	19.784	-	-	-
Water vapor resistance, Z [10^{9} Pa·m^{2}·s·kg^{-1}]	0.506	3.989	5.457	2.776
Water vapor permeability, δ [10^{-12} kg·Pa^{-1}·m^{-1}·s^{-1}]	22.844	3.049	1.788	3.768
Water vapor diffusion resistance factor, μ [-]	8.490	63.760	108.713	51.575
Water vapor diffusion-equivalent air layer thickness, S_d [m]	0.098	0.776	1.061	0.539

Among the materials tested, stone wool had the highest water vapor permeance, W_c (19.78×10^{-10} kg·Pa^{-1}·m^{-2}·s^{-1}) and permeability, δ (22.844×10^{-12} kg·Pa^{-1}·m^{-1}·s^{-1}), allowing water vapor to pass through more easily. Native poplar wood had the lowest water vapor permeability, δ (1.788×10^{-12} kg·Pa^{-1}·m^{-1}·s^{-1}) and the highest water vapor resistance, Z (5.457×10^{9} Pa·m^{2}·s ·kg^{-1}), indicating its strong resistance to water vapor transfer across the grain. After partial delignification, the water vapor permeance of poplar wood increased significantly, confirming that the removal of non-cellulosic substances

facilitates mass transfer between ambient air and materials. More water vapor was allowed to pass through the material more easily. A comparison of the water vapor resistance factor (μ) among the materials revealed that the μ of poplar wood decreased from 108.713 to 51.575 after partial delignification, similar to PIR, making it more permeable to water vapor but still more resistant than stone wool (μ = 8.49). This again demonstrated the presence of higher open porosity across the grain of gradient-delignified poplar wood. For such highly hygroscopic materials, the vapor permeability increases exponentially with a power law relationship as the ambient humidity increases due to the increase in water content [43]. This finding indicates that while delignification increases the material's permeability, it does not make it as open to vapor transfer as does stone wool. Understanding these properties allows the appropriate selection of the material for specific environmental conditions.

For anisotropic materials like wood, where liquid conduction is faster in the longitudinal direction, it is important to test in the direction of the intended application that is exposed to water vapor. Determining water vapor permeability is necessary to understand how water vapor can diffuse inside a material and potentially create zones with high relative humidity and low temperature, increasing the risk of condensation. Condensation can lead to mold growth, which can affect human health and cause long-term structural damage. To mitigate this risk, adding a vapor barrier in places where moisture levels are highest is a common practice. The thermal properties are also affected by the presence of moisture, as mentioned earlier. Thus, it is necessary to identify the water vapor permeability of new materials under different climatic conditions to perform hygrothermal simulations of walls.

3.3.3. Water Absorption Coefficient

The water absorption coefficient (A_w) indicates how quickly a material can absorb water when partially immersed, allowing for an understanding of the liquid transport properties of porous materials. This imbibition method causes capillary flow through porous structures, which can be described via Washburn's equation. Wood is a naturally porous material; when exposed to liquid water, especially above the fiber saturation point, liquid water can quickly fill the cell lumina with water [7]. Delignified wood with increased porosity requires an understanding of its liquid transport properties to ensure its long-term performance. As high water absorption can lead to dimensional instability, reduced mechanical strength, and increased risk of fungal or insect attack, it is therefore necessary to evaluate the material's behavior in the case of moisture exposure.

The resulting water absorption coefficients (A_w) of native poplar wood, gradient-delignified poplar wood, stone wool, and PIR are presented in Table 4. Figure 12 revealed that water absorption occurs in two stages: an initial rapid phase of water absorption into the pores as a result of capillary action and hydrophilicity, followed by a slower phase as the saturation point is reached. Native poplar wood, even when tested across the grain, absorbs water relatively fast. However, after wood modification, gradient-delignified wood had the highest absorption capacity, with the steepest slope in the graph, which was likely due to its higher open porosity resulting from delignification. Despite the orientation of the fibers being perpendicular to the water absorption direction, the presence of some ray cells and a new porosity facilitated water capillary movements. The first initial rapid water absorption phase could have taken place even earlier, before the first measurement (less than 5 min), resulting in a nearly vertical slope between the origin point (0,0) and the first measurement. The water absorption coefficient could have been underestimated. The presence of lignin, which is hydrophobic, moderates overall water absorption and acts as a water barrier. As non-cellulosic substances, particularly lignin, are removed, the modified wood becomes more hydrophilic and porous, facilitating

greater water uptake. The improved hygroscopicity of gradient-delignified wood was also due to its high volume of nanopores. These newly created pores, present in the cell wall of wood fibers, have nano-scale diameters, favoring the adsorption and capillary condensation of water. Regrettably, this caused the modified wood to be more susceptible to water absorption, which could be a disadvantage in moisture exposure applications, such as outdoor construction. Conventional insulation materials, such as stone wool and PIR, have very slow absorption rates, and PIR has nearly zero water absorption capacity. These materials are designed to resist water absorption, which is desirable for insulation materials used in moist environments. Thus, gradient-delignified wood may not be suitable for insulating purposes in humid environments unless it is treated or combined with hydrophobic protection layers.

Table 4. Water absorption coefficient, A_w, of various materials obtained from partial immersion.

Materials	Linear Equation $\frac{\Delta m}{S} = f(\sqrt{t})$	Coefficient of Determination, R^2	Water Absorption Coefficient, A_w [kg·m^{-2}·s$^{-0.5}$]
Stone wool	$0.28(\sqrt{t}) + 26$	0.8947	0.203
PIR	$0.07(\sqrt{t}) + 29$	0.7273	0.064
Native poplar wood (transverse direction)	$4(\sqrt{t}) + 216$	0.9998	4.018
Gradient-delignified poplar wood (transverse direction)	$7(\sqrt{t}) + 3408$	0.9908	6.769

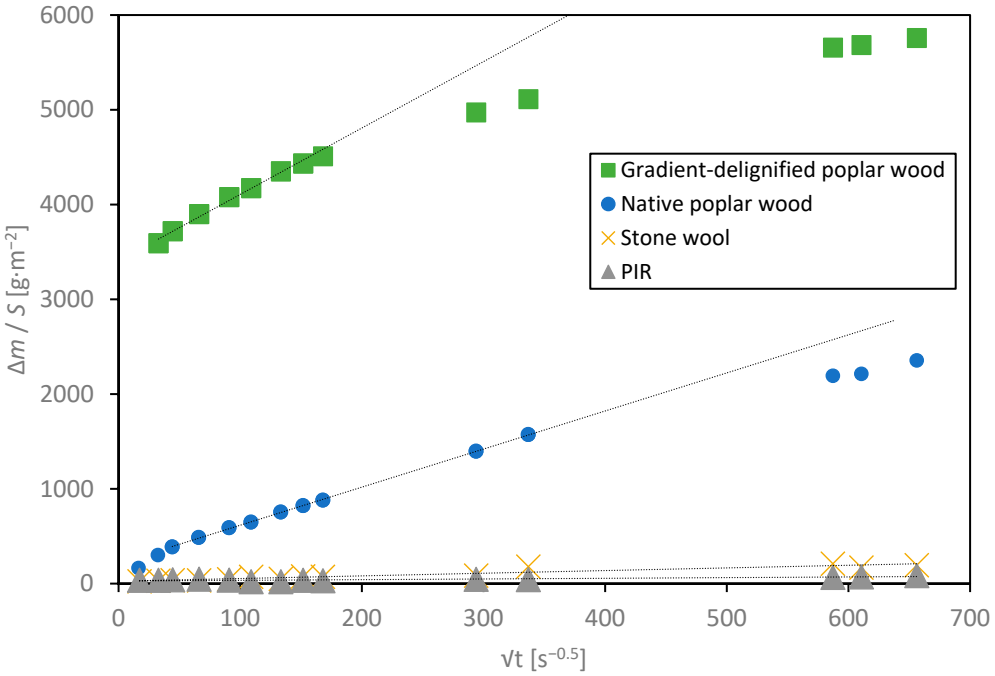


Figure 12. Water uptake by liquid water absorption vs. square root of time.

The water absorption coefficient (A_w) was then used to determine the liquid transport coefficient, D_w (m^2·s^{-1}), with the moisture storage function. The complete saturation of samples at 100% RH for the definition of free water content was difficult to measure precisely because of its exponential increase. The values used in the calculation were expected to be underestimated. Figure 13 illustrates that gradient-delignified poplar wood had a higher liquid transport coefficient than native poplar wood did, especially at higher normalized water contents. This indicated that the material had become more porous and

hydrophilic, leading to faster water transport through the gradient-delignified wood as it became saturated, even in the fibers' transverse direction.

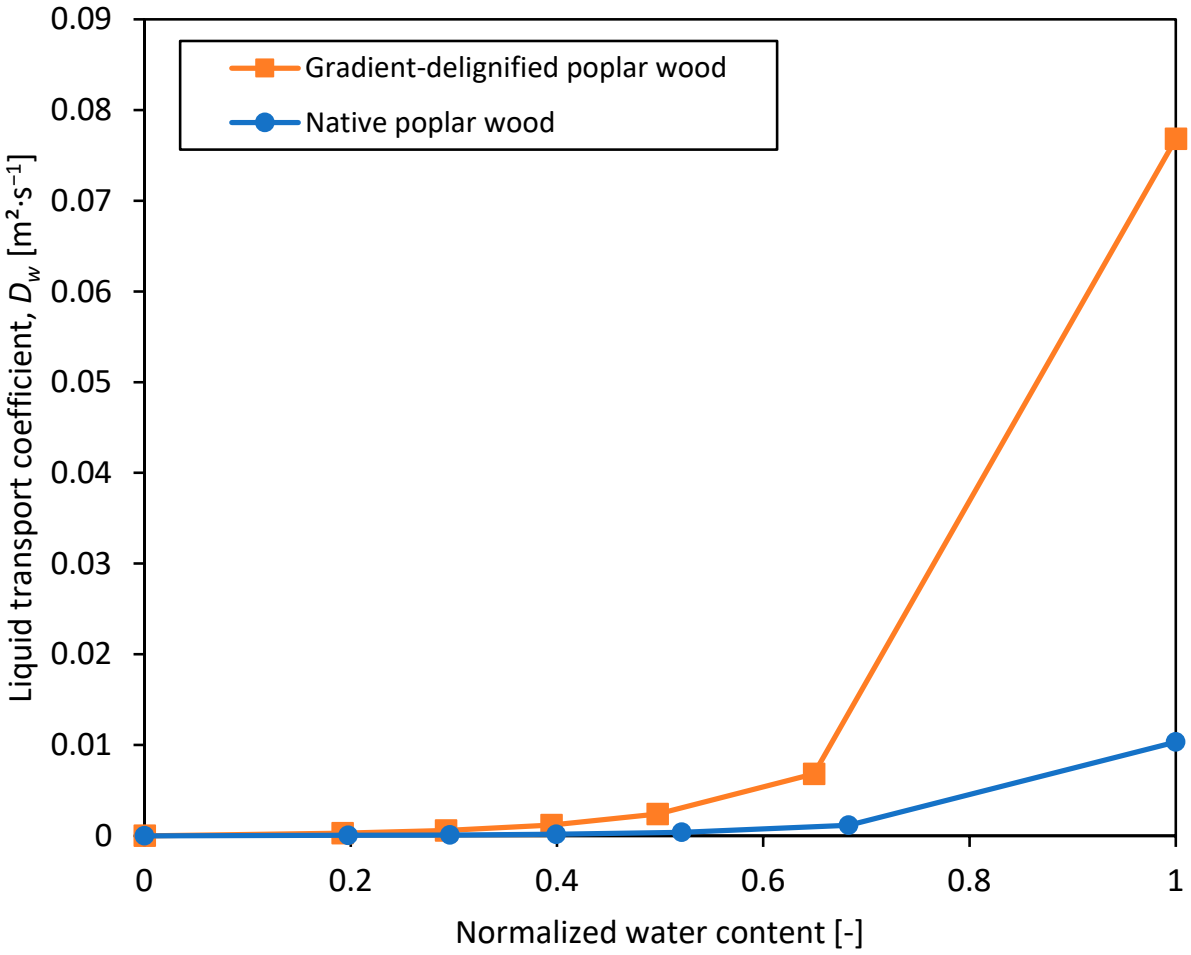


Figure 13. Liquid transport coefficients, D_w of native and gradient-delignified poplar wood.

3.4. Mechanical Properties

Wood's mechanical properties, such as strength and stiffness, usually increase with density. However, delignification leads to pore creation, a reduction in density, and consequently, a decrease in mechanical strength. Compression tests can reveal the behavior of delignified wood, particularly its compressive strength, modulus of elasticity, and stress–strain response, under different loading directions. As lignin acts as the natural binder between cellulose fibrils in wood, its absence weakens the overall structure. Additionally, delignified wood presents micron-scale cavities and nanoscale pores that develop during lignin removal, which reduces its compressive strength [44]. For example, "nanowood" has a compressive strength of 13 MPa in the axial direction, which is lower than that of natural basswood (~32.5 MPa) due to the absence of lignin [15]. Delignified wood also showed reduced stiffness, as indicated by the elastic Young's modulus of 184.9 MPa for delignified balsa wood, compared with 216 MPa for untreated balsa wood [44]. In contrast, wood foam prepared by sulphonation of pine wood, which retains lignin and hemicelluloses, has a higher Young's modulus of 344 MPa in the longitudinal direction, indicating that partial lignin retention can optimize stress transfer between cells to increase the load-bearing capacity [34,45].

The key results from the stress–strain (σ-ε) curves were summarized in terms of compressive stress at 10% strain (Figure 14) and compressive strength (Figure 15). The

compressive strength values could only be obtained in the longitudinal direction due to the occurrence of fracture stress. In contrast, the radial and tangential directions exhibited densification behavior where lumens were compressed and the fibers were densified until a maximum strain was reached, transmitting the load to the testing machine without fracturing. This densification process has the potential to make stronger materials. Densification without rupture in the transverse direction might improve the stress-bearing capacity in the longitudinal direction due to the closure of lumens and increased friction between the cell walls and cellulose fibrils.

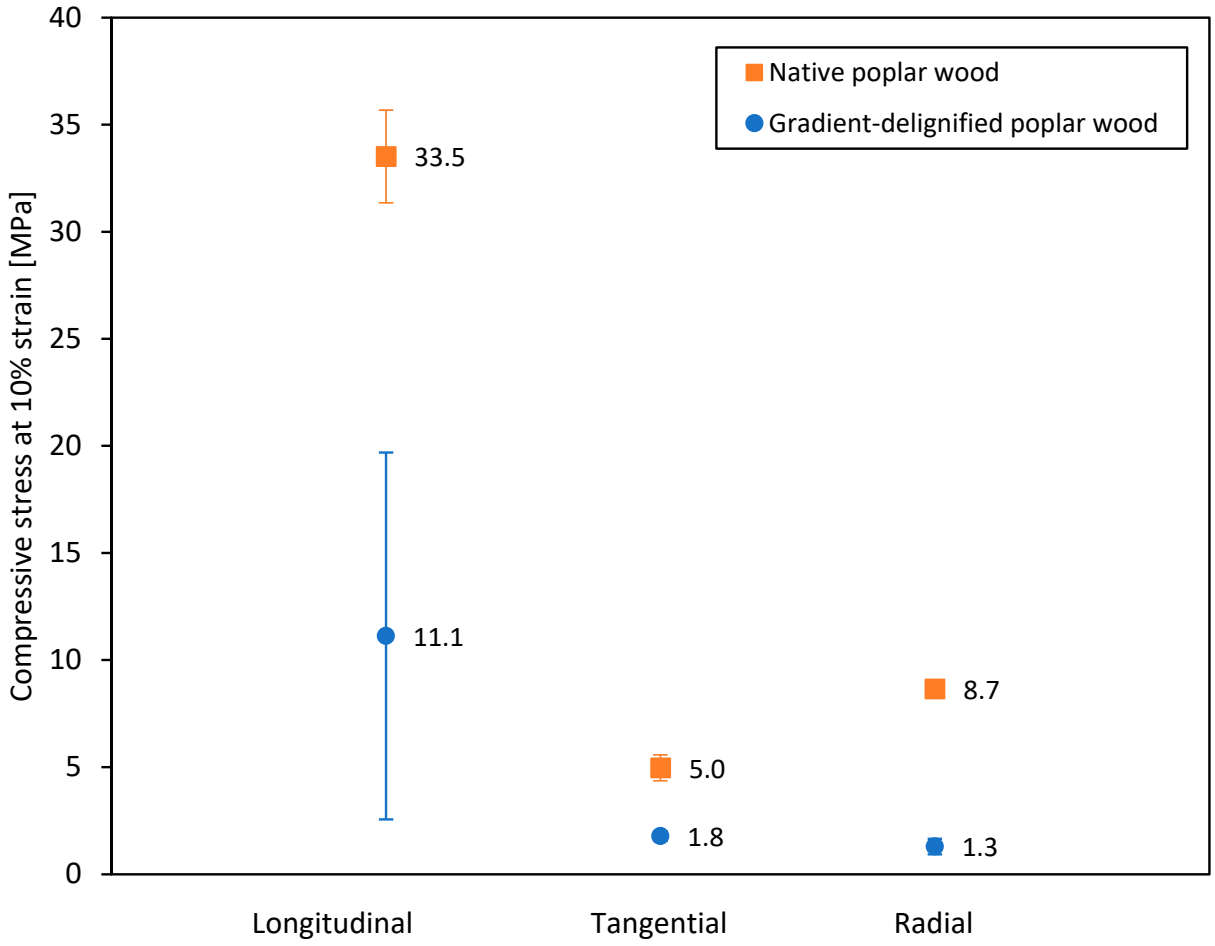


Figure 14. Compressive stress at 10% strain of native and gradient-delignified poplar wood in the L, T, and R directions (stress [MPa] ± standard deviation).

After modification, the mechanical properties of the gradient-delignified wood deteriorated. Lignin acts as an adhesive between cellulose, contributing to the overall strength and stiffness of wood. Its removal isolated cellulose microfibrils, particularly in the middle lamella and cell wall corners, reducing friction among fibrils and leading to uneven and ineffective stress transfer.

The anisotropic nature of wood, where the alignment of cellulose fibers along the longitudinal direction results in the highest mechanical properties, is evident in Figure 14. Despite partial delignification, the natural orientation and crystalline structure of cellulose were maintained, preserving strength in the longitudinal direction. However, a significant reduction in the elastic Young's modulus was observed, likely due to the decreased ability to transfer stress effectively, causing the modified wood to reach 10% strain at lower stresses. In the radial and tangential directions, the load-bearing capacity of the wood was lower due to the presence of larger lumens, particularly in earlywood. In the radial

direction, earlywood dominated the initial stress response because of its softer and more deformable cell walls. Figure 14 also shows that poplar wood experienced even greater strength loss after partial delignification. Variations in the earlywood-to-latewood ratio and inconsistencies in the uniformity of the delignification treatment likely contributed to the variability in the values of the mechanical properties among the samples. However, distinct mechanical performance deterioration can be observed in the wood after modification.

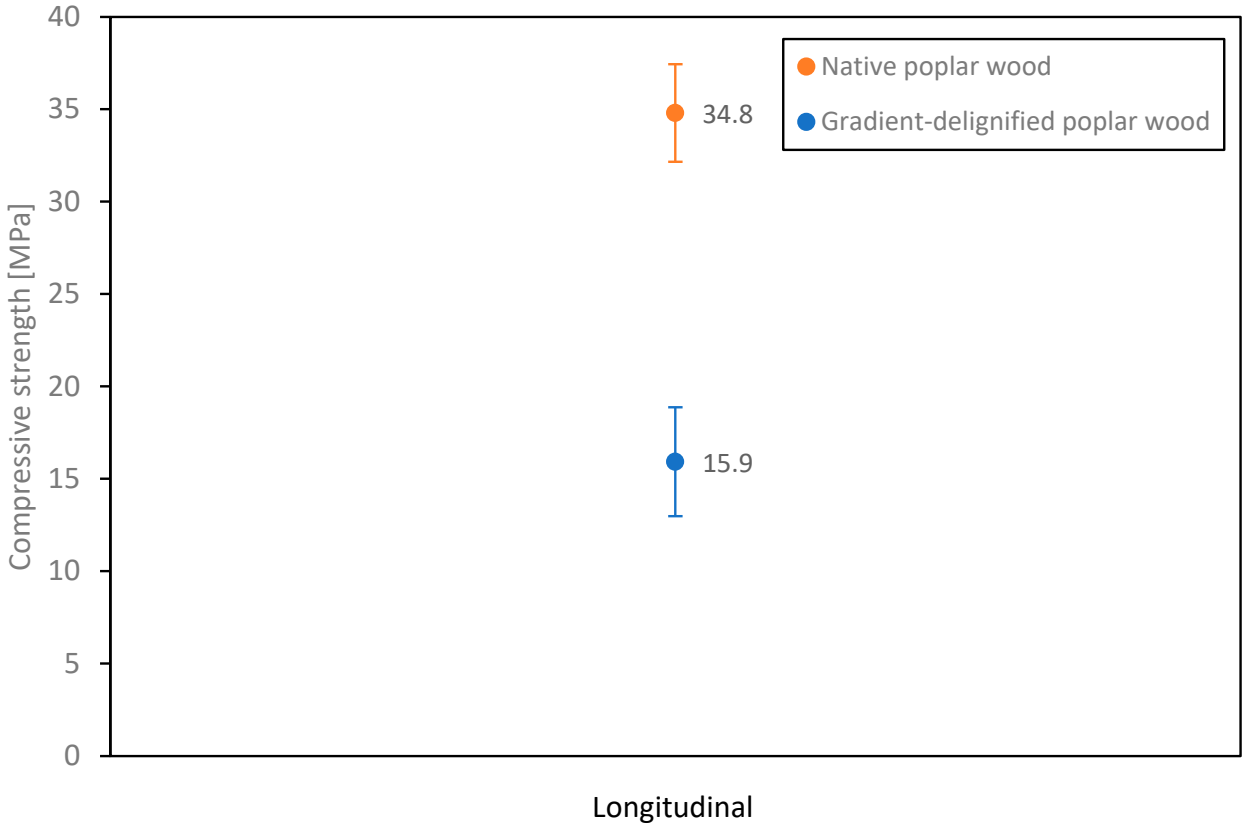


Figure 15. Compressive strength of native and gradient-delignified poplar wood in the longitudinal direction (strength [MPa] ± standard deviation).

Compared with complete delignification, partial delignification results in greater structural integrity, where the removal of non-cellulosic substances completely disrupts cellulose interactions. It is necessary to control the delignification process to retain sufficient lignin and hemicelluloses, ensuring that the wood can still withstand loads. Even drying methods can impact mechanical performance by influencing the cell wall structure, where preserving new porosities post-treatment may reduce the mechanical strength. There is a trade-off between porosity and mechanical properties. High porosity results in lower mechanical strength, whereas lower porosity enhances it. Instead of striving for optimal performance across all criteria, the focus should be on the possible applications of this pioneering modified material. For example, if anisotropy is undesirable, cross-fiber composites might create a more homogeneous material, especially for load-bearing in weaker directions. Alternatively, designs could prioritize the longitudinal direction for load-bearing, but this strategy would require considering other properties, such as thermal conductivity and water absorption, which are also higher in this direction.

Eventually, the wood density and moisture content affected the reliability of this characterization study. The density of poplar wood decreased significantly after partial delignification, explaining the reduction in mechanical properties. While parameters such as specific strength and specific elastic Young's modulus could be used for more normalized

comparisons, they are less relevant when comparing the same wood species and thus were not detailed in this study. The moisture content plays a significant role, as indicated by previous hygric characterizations. Although the samples were conditioned under the same environmental conditions, the different interactions of the modified wood with moisture likely contributed to the observed reduction in mechanical performance.

In general, the mechanical characterization results demonstrated the expected trends, particularly the significant reduction in compressive properties post-modification due to partial delignification. These findings align with the literature, which emphasized the critical role of lignin in maintaining the mechanical integrity of wood.

4. Future Research Directions

Wood is highlighted as an exceptional structural material that not only provides thermal comfort but also plays a role in reducing atmospheric CO_2 levels. The potential of wood as a sustainable alternative to synthetic thermal insulators is supported by its carbon storage ability. When the wood dimensions were increased, the laboratory-scale delignification process was inadequate, resulting in partial delignification that produced a composite material with a delignified surface and lignified core. This outcome introduced "gradient-delignified wood", which balanced the desired thermal insulating properties with the hygric and mechanical properties, although it still led to significantly increased moisture uptake and decreased mechanical strength.

This study successfully integrated a wide range of microscopic and macroscopic experimental techniques to characterize gradient-delignified wood. It was identified as a promising thermal insulator, but its tendency to defibrillate remains a significant obstacle. Exploring alternative wood species, such as fir, a low-density softwood, could offer additional insights. The variability in wood, combined with difficulties in achieving uniform delignification, introduced uncertainties. The data presented were based on a limited number of sample repetitions, which may affect the reliability of the findings. The natural heterogeneity of the wood samples and the small sample masses used in these experiments could have also reduced the precision of the results.

The thermal properties of insulating materials may vary depending on the manufacturing process, moisture content, and environmental conditions. For delignified wood, the level of delignification was found to affect the specific heat capacity. To explore the use of delignified wood in various applications, especially in building envelopes that are exposed to a wide range of temperatures (from −50 °C to +50 °C), more experimental research is needed [35]. Research should focus on determining the specific heat capacity of modified wood with different degrees of delignification. This will help in accurately predicting heat flux and verifying material performance in different climates. The study also highlighted the anisotropic nature of the thermal conductivity of wood, which makes it difficult to define the exact absolute values. Steady-state methods in all three directions for a larger sample are needed to characterize these properties fully. A proof of concept using larger samples is needed to draw more representative conclusions.

A significant challenge for gradient-delignified wood for practical applications is its high susceptibility to moisture, which affects its thermal insulation, shrink–swell properties, and mold risk. To mitigate these drawbacks, protective strategies such as impregnation with resins or hydrophobic agents are essential. The delignification process itself facilitates such impregnation, enabling the creation of new functional composite materials [46]. Alternatively, the material can be integrated as the core of sandwich panels, where impermeable metal sheets provide long-term protection. In addition, the thickness proportion of heterogeneous, gradient-delignified wood must be precisely determined to better understand its mechanical, thermal, and moisture behaviors and to ensure consistent properties. Nev-

ertheless, challenges remain due to the variability introduced by the experimental setup, specimen dimensions, and non-optimized treatment protocol.

The material properties reported in this work can serve as material data in simulations and as experimental benchmarks for validating material models. To characterize wood-based materials fully, further research is also necessary to study the influence of humidity and temperature on their mechanical properties. The limited compressive testing did not provide a complete picture of the mechanical behavior of the wood under other types of loading, such as tensile or flexural forces. The removal of lignin not only deteriorates the mechanical properties of wood but also increases the risk of defibrillation among cellulose fibrils. In addition, modified wood is more susceptible to dimensional changes during the drying process. These effects may not always be negative. In applications where flexibility is desired, such modifications could be beneficial.

The development of wood modification nanotechnology presents opportunities in fields such as photonics (transparent wood), energy storage, fire retardancy, and water purification. Nanoporous wood templates, wood aerogels, and wood xerogels offer eco-friendly alternatives for improving thermal efficiency. However, scaling up delignification for industrial production remains challenging due to technical, economic, and efficiency constraints. Industrial collaboration is needed to develop pilot production systems with large-volume reactors capable of handling the high temperatures and pressures required while ensuring cost-effectiveness. Future studies can also explore composite-based solutions, like layering delignified veneers or assembling smaller treated samples, to overcome large-scale treatment limitations while maintaining material performance consistency. Strategies to improve feasibility include optimizing process parameters, using locally sourced or aged wood, and targeting applications where gradient-delignified wood shows the highest potential.

5. Conclusions

This study demonstrates the potential of gradient-delignified wood as a sustainable thermal insulation material. By partially delignifying $100 \times 100 \times 10\ mm^3$ poplar wood boards, we produced a hybrid structure with delignified white surfaces enclosing a lignified brown core. This bio-based material preserved load-bearing capacity while improving thermal performances.

Microscopic observations revealed increased porosity, lumen deformation, and cell wall swelling at the delignified regions. From a thermal perspective, gradient-delignified wood presented higher specific heat capacity and thermal diffusivity, reduced transverse thermal conductivity, and thermal effusivity. Hygroscopic behavior was also altered, with increased moisture uptake, reduced water vapor diffusion resistance, and accelerated liquid uptake. Mechanical testing confirmed lower compressive strength compared to native wood, but the lignified core allowed the gradient-delignified wood to retain structural integrity.

These findings advance the field of wood modification nanotechnology through the development of a biodegradable, wood-based thermal insulator with properties comparable to those of synthetic materials. Beyond sustainability, this work valorizes locally abundant French poplar wood and paves the way for the innovative use of wood in engineering applications. Particularly in modular construction, gradient-delignified wood shows strong potential as a core material for sandwich panels, provided that the challenges of industrial scalability are addressed. This research contributes to the carbon footprint reduction of construction materials and supports energy-efficient building solutions.

Author Contributions: Conceptualization, Y.H.C., J.G., R.M.P., N.L. and P.B.; methodology, S.-E.O., C.V. and P.B.; formal analysis, Y.H.C., S.-E.O. and J.G.; investigation, Y.H.C.; resources, S.-E.O., C.V., R.M.P., N.L. and P.B.; writing—original draft preparation, Y.H.C.; writing—review and editing, S.-

E.O., C.V., J.G., R.M.P., N.L. and P.B.; visualization, Y.H.C.; supervision, S.-E.O., C.V., R.M.P., N.L. and P.B.; project administration, J.G. and P.B.; funding acquisition, J.G., R.M.P., N.L. and P.B. All authors have read and agreed to the published version of the manuscript.

Funding: This research was funded by the French National Research Agency (ANR) and the company Dagard, under the France Relance plan.

Data Availability Statement: The original contributions presented in the study are included in the article, further inquiries can be directed to the corresponding author.

Acknowledgments: The authors are grateful to Y. Horikawa for valuable guidance on wood delignification protocols. The authors also thank C. Blavignac, A. Nouviaire, F. Gros, F. Brun, F. Audonnet, and C. Gardarin for their assistance with the experimental instruments.

Conflicts of Interest: Authors Yi Hien Chin and Nicolas Labonne were employed by the company Dagard. The remaining authors declare that the research was conducted in the absence of any commercial or financial relationships that could be construed as a potential conflict of interest.

Abbreviations

The following abbreviations are used in this manuscript:

DVS	Dynamic vapor sorption
PIR	Polyisocyanurate
RH	Relative humidity
SEM	Scanning electron microscopy

References

1. Tlaiji, G.; Biwole, P.; Ouldboukhitine, S.; Pennec, F. A Mini-Review on Straw Bale Construction. *Energies* **2022**, *15*, 7859. [CrossRef]
2. Zhao, X.; Liu, Y.; Zhao, L.; Yazdkhasti, A.; Mao, Y.; Siciliano, A.P.; Dai, J.; Jing, S.; Xie, H.; Li, Z.; et al. A scalable high-porosity wood for sound absorption and thermal insulation. *Nat. Sustain.* **2023**, *6*, 306–315. [CrossRef]
3. Schulte, M.; Lewandowski, I.; Pude, R.; Wagner, M. Comparative life cycle assessment of bio-based insulation materials: Environmental and economic performances. *GCB Bioenergy* **2021**, *13*, 979–998. [CrossRef]
4. Bakkour, A.; Ouldboukhitine, S.-E.; Biwole, P.; Amziane, S. A review of multi-scale hygrothermal characteristics of plant-based building materials. *Constr. Build. Mater.* **2024**, *412*, 134850. [CrossRef]
5. He, S.; Chen, C.; Li, T.; Song, J.; Zhao, X.; Kuang, Y.; Liu, Y.; Pei, Y.; Hitz, E.; Kong, W.; et al. An Energy-Efficient, Wood-Derived Structural Material Enabled by Pore Structure Engineering towards Building Efficiency. *Small Methods* **2020**, *4*, 1900747. [CrossRef]
6. Gérard, J.; Guibal, D.; Paradis, S.; Vernay, M.; Beauchêne, J.; Brancheriau, L.; Châlon, I.; Daigremont, C.; Détienne, P.; Fouquet, D.; et al. *Tropix*, version 7; CIRAD: Montpellier, France, 2011; 25 MB. [CrossRef]
7. Forest Products Laboratory (Ed.) *Wood Handbook: Wood as an Engineering Material*, Centennial ed.; General technical report/United States Department of Agriculture, Forest Service, Forest Products Laboratory; Forest Products Laboratory, U.S. Department of Agriculture, Forest Service: Madison, WI, USA, 2010; ISBN 978-1-4848-5970-4.
8. Keplinger, T.; Wittel, F.K.; Rüggeberg, M.; Burgert, I. Wood Derived Cellulose Scaffolds—Processing and Mechanics. *Adv. Mater.* **2021**, *33*, 2001375. [CrossRef] [PubMed]
9. Segmehl, J.S. Wood and Wood-Derived Cellulose Scaffolds for the Preparation of Multi-Functional Materials. Ph.D. Thesis, ETH Zurich, Zurich, Switzerland, 2017; p. 190.
10. Yano, H.; Hirose, A.; Collins, P.J.; Yazaki, Y. Effects of the removal of matrix substances as a pretreatment in the production of high strength resin impregnated wood based materials. *J. Mater. Sci. Lett.* **2001**, *20*, 1125–1126. [CrossRef]
11. Kumar, A.; Jyske, T.; Petrič, M. Delignified Wood from Understanding the Hierarchically Aligned Cellulosic Structures to Creating Novel Functional Materials: A Review. *Adv. Sustain. Syst.* **2021**, *5*, 2000251. [CrossRef]
12. Terzopoulou, P.; Vouvoudi, E.C.; Achilias, D.S. Delignification as a Key Strategy for Advanced Wood-Based Materials: Chemistry, Delignification Parameters, and Emerging Applications. *Forests* **2025**, *16*, 993. [CrossRef]
13. Li, J.; Chen, C.; Zhu, J.Y.; Ragauskas, A.J.; Hu, L. In Situ Wood Delignification toward Sustainable Applications. *Acc. Mater. Res.* **2021**, *2*, 606–620. [CrossRef]
14. Jelle, B.P. Traditional, state-of-the-art and future thermal building insulation materials and solutions—Properties, requirements and possibilities. *Energy Build.* **2011**, *43*, 2549–2563. [CrossRef]

15. Li, T.; Song, J.; Zhao, X.; Yang, Z.; Pastel, G.; Xu, S.; Jia, C.; Dai, J.; Chen, C.; Gong, A.; et al. Anisotropic, lightweight, strong, and super thermally insulating nanowood with naturally aligned nanocellulose. *Sci. Adv.* **2018**, *4*, eaar3724. [CrossRef]
16. Chen, Z.; Dang, B.; Luo, X.; Li, W.; Li, J.; Yu, H.; Liu, S.; Li, S. Deep Eutectic Solvent-Assisted In Situ Wood Delignification: A Promising Strategy To Enhance the Efficiency of Wood-Based Solar Steam Generation Devices. *ACS Appl. Mater. Interfaces* **2019**, *11*, 26032–26037. [CrossRef] [PubMed]
17. Garemark, J.; Perea-Buceta, J.E.; Rico del Cerro, D.; Hall, S.; Berke, B.; Kilpeläinen, I.; Berglund, L.A.; Li, Y. Nanostructurally Controllable Strong Wood Aerogel toward Efficient Thermal Insulation. *ACS Appl. Mater. Interfaces* **2022**, *14*, 24697–24707. [CrossRef]
18. Wang, S.; Li, L.; Zha, L.; Koskela, S.; Berglund, L.A.; Zhou, Q. Wood xerogel for fabrication of high-performance transparent wood. *Nat. Commun.* **2023**, *14*, 2827. [CrossRef]
19. Horikawa, Y.; Tsushima, R.; Noguchi, K.; Nakaba, S.; Funada, R. Development of colorless wood via two-step delignification involving alcoholysis and bleaching with maintaining natural hierarchical structure. *J. Wood Sci.* **2020**, *66*, 37. [CrossRef]
20. Song, J.; Chen, C.; Yang, Z.; Kuang, Y.; Li, T.; Li, Y.; Huang, H.; Kierzewski, I.; Liu, B.; He, S.; et al. Highly Compressible, Anisotropic Aerogel with Aligned Cellulose Nanofibers. *ACS Nano* **2018**, *12*, 140–147. [CrossRef] [PubMed]
21. Jin, Y.; Tian, F.; She, Y.; Xu, H.; Zhu, C.; Wu, Y.; Chen, H.; Wang, B.; Xu, X. Thermal Insulation Properties of Delignified Balsa and Paulownia Wood "Foams" with Polylactic Acid Coverings. *Forests* **2023**, *14*, 2339. [CrossRef]
22. Barbosa, K.T.; Cardoso, G.V.; Pereira Acosta, A.; Aramburu, A.B.; Delucis, R.D.A.; Gatto, D.A.; Labidi, J.; Beltrame, R. Unveiling the Potential of Brazilian Eucalyptus for Transparent Wood Manufacturing via the Kraft Pulping Process as a Future Building Material. *Forests* **2024**, *15*, 1544. [CrossRef]
23. Kurei, T.; Tsushima, R.; Okahisa, Y.; Nakaba, S.; Funada, R.; Horikawa, Y. Creation and Structural Evaluation of the Three-Dimensional Cellulosic Material "White-Colored Bamboo". *Holzforschung* **2021**, *75*, 180–186. [CrossRef]
24. Chin, Y.H.; Horikawa, Y.; Vial, C.; Gril, J.; Moutou Pitti, R.; Ouldboukhitine, S.-E.; Labonne, N.; Biwole, P. A scalable solvent-exchange strategy for the drying of colorless Japanese cedar (*Cryptomeria japonica*). *Dry. Technol.* **2024**, *43*, 510–526. [CrossRef]
25. Kollmann, F.F.P.; Côté, W.A. *Principles of Wood Science and Technology*; Springer: Berlin/Heidelberg, Germany, 1968; ISBN 978-3-642-87930-2.
26. Jannot, Y.; Degiovanni, A.; Félix, V.; Bal, H. Measurement of the thermal conductivity of thin insulating anisotropic material with a stationary hot strip method. *Meas. Sci. Technol.* **2011**, *22*, 035705. [CrossRef]
27. Adl-Zarrabi, B.; Boström, L.; Wickström, U. Using the TPS method for determining the thermal properties of concrete and wood at elevated temperature. *Fire Mater.* **2006**, *30*, 359–369. [CrossRef]
28. *NF EN ISO 12572*; Hygrothermal Performance of Building Materials and Products—Determination of Water Vapour Transmission Properties—Cup Method. AFNOR: Saint-Denis, France, 2016.
29. *NF EN 12086*; Thermal Insulating Products for Building Applications—Determination of Water Vapour Transmission Properties. AFNOR: Saint-Denis, France, 2013.
30. *NF EN ISO 15148*; Hygrothermal Performance of Building Materials and Products—Determination of Water Absorption Coefficient by Partial Immersion. AFNOR: Saint-Denis, France, 2003.
31. *NF EN 826*; Thermal Insulating Products for Building Applications—Determination of Compression Behaviour. AFNOR: Saint-Denis, France, 2013.
32. Fu, Q.; Medina, L.; Li, Y.; Carosio, F.; Hajian, A.; Berglund, L.A. Nanostructured Wood Hybrids for Fire-Retardancy Prepared by Clay Impregnation into the Cell Wall. *ACS Appl. Mater. Interfaces* **2017**, *9*, 36154–36163. [CrossRef] [PubMed]
33. Li, Y.; Fu, Q.; Yu, S.; Yan, M.; Berglund, L. Optically Transparent Wood from a Nanoporous Cellulosic Template: Combining Functional and Structural Performance. *Biomacromolecules* **2016**, *17*, 1358–1364. [CrossRef]
34. Kurei, T.; Sakai, S.; Nakaba, S.; Funada, R.; Horikawa, Y. Structural and mechanical roles of wood polymer assemblies in softwood revealed by gradual removal of polysaccharides or lignin. *Int. J. Biol. Macromol.* **2024**, *259*, 129270. [CrossRef] [PubMed]
35. Yousefi, Y.; Tariku, F. Thermal Conductivity and Specific Heat Capacity of Insulation materials at Different Mean Temperatures. *J. Phys. Conf. Ser.* **2021**, *2069*, 012090. [CrossRef]
36. Nocentini, K. Comportement Thermo-Hygrique de Blankets Aérogels de Silice et Applications à L'isolation des Bâtiments. Matériaux. Ph.D. Thesis, Université Paris Sciences et Lettres, Paris, France, 2018.
37. Hemingway, B.S.; Robie, R.A. *Heat Capacity of Polystyrene from 275 to 315 K*; UNITED STATES DEPARTMENT OF THE INTERIOR, U.S. GEOLOGICAL SURVEY: Reston, VA, USA, 1994.
38. Hunt, J.; Gu, H. Finite Element Analyses of Two Dimensional, Anisotropic Heat Transfer in Wood. In Proceedings of the 2004 International ANSYS Conference, Pittsburgh, PA, USA, 24–26 May 2004.
39. Busquets-Ferrer, M.; Czabany, I.; Vay, O.; Gindl-Altmutter, W.; Hansmann, C. Alkali-extracted tree bark for efficient bio-based thermal insulation. *Constr. Build. Mater.* **2021**, *271*, 121577. [CrossRef]
40. Hu, L.; Li, T.; He, S.; Song, J.; Chen, C. Delignified Wood Materials, and Methods for Fabricating and Use Thereof. U.S. Patent US20200238565A1, 30 July 2020.

41. Grönquist, P.; Frey, M.; Keplinger, T.; Burgert, I. Mesoporosity of Delignified Wood Investigated by Water Vapor Sorption. *ACS Omega* **2019**, *4*, 12425–12431. [CrossRef]
42. Montanari, C.; Olsén, P.; Berglund, L.A. Interface tailoring by a versatile functionalization platform for nanostructured wood biocomposites. *Green Chem.* **2020**, *22*, 8012–8023. [CrossRef]
43. Galbraith, G.H.; McLean, R.C.; Guo, J. Moisture permeability data presented as a mathematical function applicable to heat and moisture transport models. *Build. Simul.* **1997**, *5*, 301–305.
44. Fu, Q.; Ansari, F.; Zhou, Q.; Berglund, L.A. Wood Nanotechnology for Strong, Mesoporous, and Hydrophobic Biocomposites for Selective Separation of Oil/Water Mixtures. *ACS Nano* **2018**, *12*, 2222–2230. [CrossRef] [PubMed]
45. Mastantuoni, G.G.; Tran, V.C.; Garemark, J.; Dreimol, C.H.; Engquist, I.; Berglund, L.A.; Zhou, Q. Rationally designed conductive wood with mechanoresponsive electrical resistance. *Compos. Part Appl. Sci. Manuf.* **2024**, *178*, 107970. [CrossRef]
46. Berglund, L.A.; Burgert, I. Bioinspired Wood Nanotechnology for Functional Materials. *Adv. Mater.* **2018**, *30*, 1704285. [CrossRef] [PubMed]

Disclaimer/Publisher's Note: The statements, opinions and data contained in all publications are solely those of the individual author(s) and contributor(s) and not of MDPI and/or the editor(s). MDPI and/or the editor(s) disclaim responsibility for any injury to people or property resulting from any ideas, methods, instructions or products referred to in the content.